An improved coastal upwelling index from sea surface temperature using satellite-based approach – The case of the Canary Current upwelling system

Article *in* Continental Shelf Research · June 2014

DOI: 10.1016/j.csr.2014.03.012

CITATIONS
177

READS
3,036

8 authors, including:

Aissa Benazzouz
Institut Supérieur d'Études Maritimes Casablanca
35 PUBLICATIONS **407** CITATIONS
SEE PROFILE

Soumia Mordane
University of Hassan II of Casablanca
62 PUBLICATIONS **380** CITATIONS
SEE PROFILE

Abdellatif Orbi
58 PUBLICATIONS **1,058** CITATIONS
SEE PROFILE

Mohamed Chagdali
Université Hassan II de Casablanca
61 PUBLICATIONS **402** CITATIONS
SEE PROFILE

Continental Shelf Research ■ (■■■■) ■■■–■■■

Contents lists available at ScienceDirect

Continental Shelf Research

journal homepage: www.elsevier.com/locate/csr

Research papers

An improved coastal upwelling index from sea surface temperature using satellite-based approach – The case of the Canary Current upwelling system

Benazzouz Aïssa [a,b,*], Mordane Soumia [a], Orbi Abdellatif [b], Chagdali Mohamed [a], Hilmi Karim [b], Atillah Abderrahman [c], Lluís Pelegrí Josep [d], Demarcq Hervé [e,**]

[a] Faculté des Sciences Ben M'Sik, Avenue Idriss El Harti, Sidi Othman, BP 7955, Casablanca, Morocco
[b] Institut National de Recherche Halieutique, Boulevard Sidi Abderhamanne, BP 20030, Casablanca, Morocco
[c] Centre Royal de Télédétection Spatiale, Angle Avenue Sanawbar et Avenue Allal El Fassi, Quartier Hay Riad Rabat, Morocco
[d] Departament d'Oceanografia Física, Institut de Ciències del Mar, CMIMA-CSIC 08003, Barcelona, Spain
[e] Institut de Recherche pour le Développement, EME Research Unit, IRD, IFREMER & Univ. Montpellier II, Avenue Jean Monnet, BP 171 34203, Sète Cedex, France

ARTICLE INFO

Article history:
Received 3 August 2013
Received in revised form
19 March 2014
Accepted 24 March 2014

Keywords:
Coastal upwelling
Coastal upwelling index
Canary upwelling system
West Africa
Sea surface temperature
Remote sensing

ABSTRACT

A new methodology to derive an SST-based upwelling index was based on a rigorous spatial analysis of satellite SST fields and their variability, by referring to previous works, from Wooster et al. (1976), Santos et al. (2011). The data was precautiously processed by considering data quality aspects (including cloud cover) and the best way to derive accurate coastal SST and its offshore reference. The relevance of the developed index was evaluated by comparing its spatial and seasonal consistency against two wind-based indices as well as with the previous SST-based indices, largely superseding these later ones in term of overall quality and spatio-temporal dynamic. Our index adequately describes the spatio-temporal variability of the coastal upwelling intensity in the Canary Current upwelling system and has the advantage of describing complementary aspects of the coastal dynamics of the region that were not covered by Ekman-based indices.

The proposed methodology is generic and can be easily applicable to various coastal upwelling systems, especially the four major eastern boundary upwelling ecosystems.

1. Introduction

Eastern Boundary Upwelling Ecosystems (EBUEs) extend over temperate and tropical regions and include some of the most productive ecosystems in the world (Carr and Kearns, 2003). Oceanography of EBUEs is forced by the equatorward trade winds that lead to the upward pumping of cold intermediate water. The phenomenon can distinctively be identified by seasonally variable low sea surface temperature (SST) and nutrient-rich water in coastal area, compared to the average SST at the same latitude (Wooster et al., 1976).

The high primary productivity of coastal upwelling systems (Herbland and Voituriez, 1974; Minas et al., 1982) sustains large fisheries of small pelagic species, a major economic resource that contributes to 20% of the global fish production for less than 3% of the world oceans surface (Ryther, 1969; Cushing, 1971; Fréon et al. 2009a).

The Canary Current Upwelling System, that extends from the Iberian Peninsula (43°N) to the south of Senegal (8°N, Fig. 1), is one of the world's four major EBUEs (Barton, 1998; Arístegui et al., 2009). The seasonal variability of the trade winds between winter and summer (Fig. 2a) induces pronounced coastal SST anomalies (Fig. 2b) with a high seasonal variability, mainly in the southern part of the system (Fig. 2b), first described by Wooster et al. (1976) based on historical measurements, wind stress and currents from on-board observations.

As described by Ekman (1905) and later by Bakun (1973), the cool and rich upwelled water along the coastal shelf edge is a consequence of the alongshore trade wind forcing. The strength and position of the wind depends on the latitudinal migration of the Intertropical Convergence Zone (ITCZ) and the associated Azores High pressure area, both oscillating between their northermost and southernmost positions in summer/winter respectively (Fig. 1), generating a seasonal wind and SST pattern (Wooster et al., 1976; Mittelstaedt, 1991; Nykjær and Van Camp, 1994; Van Camp et al., 1991).

The wind vectors from the CCMP (Cross-Calibration Multi-platform) dataset (Fig. 2a) shows a variable wind circulation between winter and summer. The coastal region is characterized by upwelling

* Corresponding author at: Institut National de Recherche Halieutique, Boulevard Sidi Abderhamanne, BP 20030, Casablanca, Morocco.
Tel.: +212 522 940771; fax: +212 522 940695.
** Corresponding author. Tel.: +33 499 573 213; fax: +33 499 573 295.
E-mail addresses: benazzouz.inrh@gmail.com (B. Aïssa), herve.demarcq@ird.fr (D. Hervé).

http://dx.doi.org/10.1016/j.csr.2014.03.012
0278-4343/

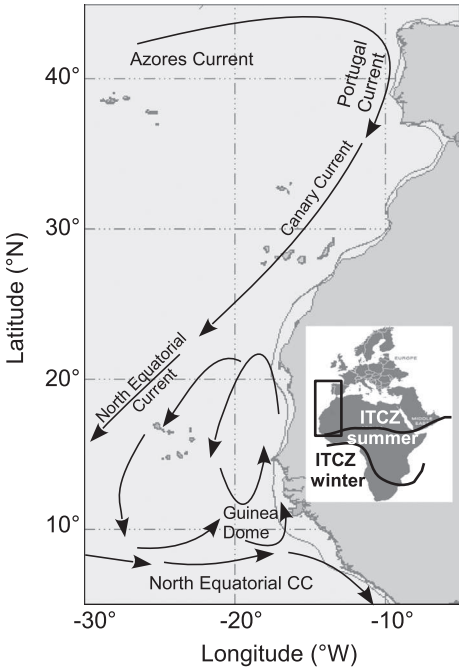

Fig. 1. Study area, including the Iberian Peninsula and the North-west African region with the main surface currents: Azores, Portugal, Canary, North Equatorial current and North Equatorial counter-current. The 200 m isobath is superimposed.

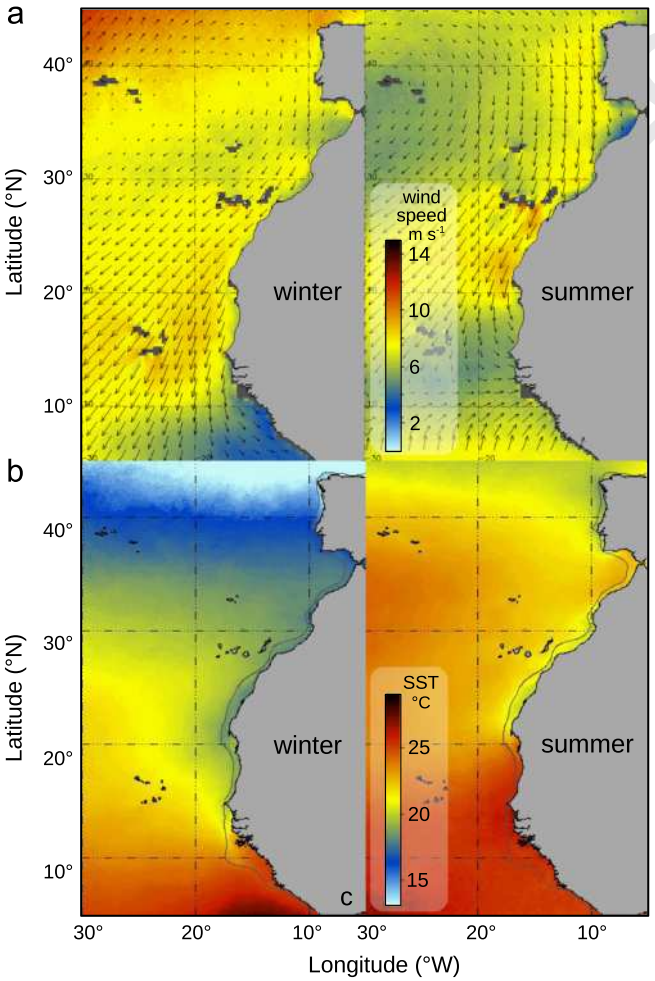

Fig. 2. Climatological means of (a) the surface wind field from QuikSCAT (1999–2009), (b) the SST from AVHRR (1982–2011) in winter (week 02–09 February) and summer (week 04–11 July), with the 200 m isobath superimposed.

favorable wind stress all year-round (Bakun and Nelson, 1991), with maximum values during summer north to 21°N and during winter south to 21°N (Mittelstaedt, 1991).

In most of the study area (10–30°N), the near-surface wind is under influence of northeast trade wind, as part of the lower part of the Hadley circulation cell. North of 30°N the exact position of a zonal belt of high pressure cells is predominantly determined by the location of the Azores High and is characterized by low north-easterly surface winds (Benazzouz, 2014). South of 15°N the ITCZ – the meridional convergence of the northeast and southeast trade winds – becomes the main driver of the upwelling seasonality.

In the Iberian Peninsula (37–43°N), equatorward winds dominate from early June to late September and generate an equatorward mean upwelling surface flow associated to the Portugal surface current (Mittelstaedt, 1991).

The physical -and classic- way of quantifying the upwelling intensity is by computing the Coriolis forces that induces the Cross-Shore Ekman transport (CSET). The wind-based "Coastal upwelling index" can be interpreted as the water flux theoretically transported offshore by the wind stress from the coastal upward flux of colder water, assuming an infinite ocean (Ekman, 1905). Consequently, this upwelling index do not consider bathymetricy of the continental shelf and therefore cannot render the complexity of the two dimensional spatial structure of the upwelling such as coastal upwelling cells, cape effects and filaments.

Another limitation in the computation of wind-based upwelling indices is the relatively short length (< 20 years) of time series available, excepting of composite products such as the CCMP Ocean surface winds, available from July 1987.

Satellite-derived SST provides a quantitative and synoptic overview of thermal features in the ocean, including the wind-driven coastal SST. The surface cooling from the upwelled water reaching the sea surface is therefore a potential proxy of the upwelling intensity.

Surface wind flux and coastal SST are two complementary parameters to quantify the spatial extent and intensity of the upwelling process at synoptic scale, the first one from a physical theory and the second one based from direct observation. The mixing of the cold upwelled water flux with the warmer surrounding surface water by turbulent mixing should be taken into account as well as the understanding of the causal mechanism of the SST variability from the wind flux. Because of their intrinsic links, Ekman transport and the resulting SST anomaly can be used as complementary variables to investigate the status of the upwelling.

The aim of the paper is to develop a new methodology to compute an improved SST-based upwelling index, applicable for all EBUEs. A review of various methods based on satellite and wind to quantify upwelling dynamics is conducted. Moreover, some of past studies concerned both the spatial structure of upwelling (e.g., fronts, eddies, filaments) and its fluctuations on synoptic to interannual time-scales (e.g., Van Camp et al., 1991; Nykjaer and Van Camp, 1994; Kostianoy and Zatsepin, 1996; Demarcq and Faure 2000; Santos et al., 2005; Nieto et al. 2012) in less than 20-year time series. Several satellite SST data series in EBUEs are available at a suitable spatio-temporal resolution (< 10 km and 1 month) and in a continuous coverage and synoptic monitoring. We used a 30 year (1981–2011) time series of 8-day global SST with the aim of synthesizing more spatially detailed information than the past works. Q3

2. Datasets

We use two homogeneous data sets from spatial observation: a 30 years sea surface temperature (SST) series from the AVHRR (Advanced Very High Resolution Radiometer) and two wind data series, respectively the SeaWind sensor and the global wind CCMP

Please cite this article as: Aïssa, B., et al., An improved coastal upwelling index from sea surface temperature using satellite-based approach –.... Continental Shelf Research (2014), http://dx.doi.org/10.1016/j.csr.2014.03.012

product which combined from all sensors available from July 1987 until today.

2.1. Pathfinder SST

We use the pathfinder AVHRR SST data set version 5.2 for the time period September 1981 to December 2011, and its corresponding 30 years climatology. Visual tests between day-time and night-time images have not shown significant differences in 8-day averages and the day-time time series has been chosen for the analysis.

This dataset is developed jointly by the University of Miami Rosenstiel School of Marine and Atmospheric Science and the NOAA National Oceanographic Data Center (NODC) from the original data of the AVHRR sensor and distributed in several formats at a spatial resolution of 4 km (see http://www.nodc.noaa.gov/sog/pathfinder4km/).

Because temporal averaging provides increased spatial coverage at the expense of temporal resolution (Campbell et al., 1995), several time series have been generated from daily data at 3, 5, 8 and 15 days, in order to test the effect of the time averaging on the SST fields quality as well as the ability to derive reliable SST-based upwelling indices.

The 8-day data set, widely used by the scientific community, is chosen as a compromise between the variability of the SST and the necessity to provide a continuous spatio-temporal coverage.

Cloud cover is the primary limitation of the SST data (McClain et al., 1992). The pathfinder SST data set is provided with a 8-level quality flag index (Kilpatrick et al., 2001). We chose the level 3 as a compromise to avoid numerous pixels of cold coastal water to be flagged because of the "reference test" that consider a maximum de departure of 2.0 °C from the DOISSTv2 climatology (Reynolds et al., 2007).

Typical thermal fields are shown for the Moroccan region (Fig. 3, left panel) and the Senegalese–Mauritanian region (right panel), respectively during summer (August) and late winter (March). Both examples correspond to the maximum upwelling intensity and spatial extension and highlight the thermal contrast between the coast and the open ocean. It also shows the lack of data caused by the inadequate cloud mask in a narrow coastal band.

2.2. QuikSCAT wind

A description of the SeaWinds scatterometer on the QuikSCAT satellite is given by Freilich et al. (1994). The scanning microwave radar infers the surface wind stress from measurements of backscatter from the roughness of the sea surface at multiple antenna look angles (Naderi et al., 1991). The wind data were extracted from the ftp://podaac.jpl.nasa.gov database and remapped into $0.25^\circ \times 0.25^\circ$ cells.

A 10-year time series (July 1999–2009) of daily-averaged wind velocity components at 10 m above the surface is extracted from the HDF (Hiearchical Data Format) files.

2.3. CCMP wind

The Cross-Calibrated, Multi-Platform Ocean Surface Wind Velocity project (hereafter, CCMP), funded under the NASA Earth Science Enterprise, is an ocean surface wind data set that use a variational analysis method (Atlas et al., 2009) to combine wind measurements derived from scatterometers (as SeaWinds on QuikSCAT and ADEOS-II, NSCAT, etc.) and microwave sensors as AMSRE on Aqua, TRMM on TMI and SSM/I and SSMIS on DMSP platforms. By combining these measurements, a consistent data record of high resolution (25 km) ocean surface winds was created for the period from July 1987 to December 2011.

2.4. North Atlantic Oscillation

The North Atlantic Oscillation index (NAO), defined as the normalized sea level pressure difference between Azores and Iceland, is used to evaluate its possible link with our upwelling index. The NAO is considered as the most important mode of variability in the northern hemisphere atmospheric circulation and is consequently supposed to be related to the strength of the westerly winds blowing across the North Atlantic Ocean. The monthly NAO index series were taken from Hurrel (1995, 1996) at the U.S. National Center for Environmental Prediction/National Center for Atmospheric Research (NCEP/NCAR) Reanalysis Project.

3. Methods

To investigate the average seasonal cycle of the SST, an 8-day climatological year is constructed from the 8-day data series from September 1981 to December 2011.

Two similar 8-day surface wind climatologies are constructed from both QuikSCAT and CCMP winds products by averaging daily images respectively from July 1999 to October 2009 and January 1988 to December 2011.

3.1. Ekman-based upwelling index processing

The Cross-Shore Ekman Transport (hereafter CSET) based on the Ekman theory (Ekman, 1905; Bakun, 1973) is computed using daily wind measurements separately from QuickSCAT and CCMP winds at forth degree resolution. Because no valid measurement is possible in the first pixel row from the coast and for most pixels of the second row, the computation is done from the band of 75–150 km off the coast, which is the closest good quality wind stress data from the coast derived from both QuikSCAT and CCMP. The angle of the coast line is computed separately from each forth degree wind measurement cell using the average direction of the 200 m isobath over a distance of three adjacent cells (about 80 km).This isobath is extracted from the ETOPO1 data base. The drag coefficient of the wind on the sea surface is computed from the non linear formula proposed by Trenberth et al. (1990).

The spatial and seasonal variability of the wind stress (Fig. 4a) and the derived CSET (Fig. 4b) shows a general increase of the upwelling from north to south that induce distinct upwelling seasons along the coast, as previously described by several authors (Wooster et al., 1976; Speth et al. 1978). From 10°N to 20°N the upwelling occurs during winter and spring, exhibiting a very strong seasonality, that progressively decreases in duration from South to North. The central region of the Northwest African upwelling (21–26°N) is characterized by a quasi-permanent upwelling, and further north marked by a strongly seasonal upwelling from April to September (Hagen, 1981; Mittelstaedt, 1991; Peters, 1976). In Portugal (37–43°N), the upwelling is very seasonal from June to August (Wooster et al., 1976; Speth et al., 1978; Fiuza et al., 1982).

3.2. Spatial structure identification and computation procedures of coastal indices from SST fields (CUI_{SST})

Historically, most SST-based upwelling indices have been taken as a simple thermal difference (ΔT) between the coastal and the offshore SST taken at the same latitude, in order to quantify the coastal cooling effect of the upwelling (Wooster et al., 1976; Nykjaer and Van Camp, 1994). Another normalized coastal upwelling index have been developed by Demarcq and Faure (2000). However, this index is difficult to define for the latitudinally changing patterns of the west African region, where different water masses occur, the SACW and NACW, respectively the South and North Atlantic Central

Please cite this article as: Aïssa, B., et al., An improved coastal upwelling index from sea surface temperature using satellite-based approach –.... Continental Shelf Research (2014), http://dx.doi.org/10.1016/j.csr.2014.03.012

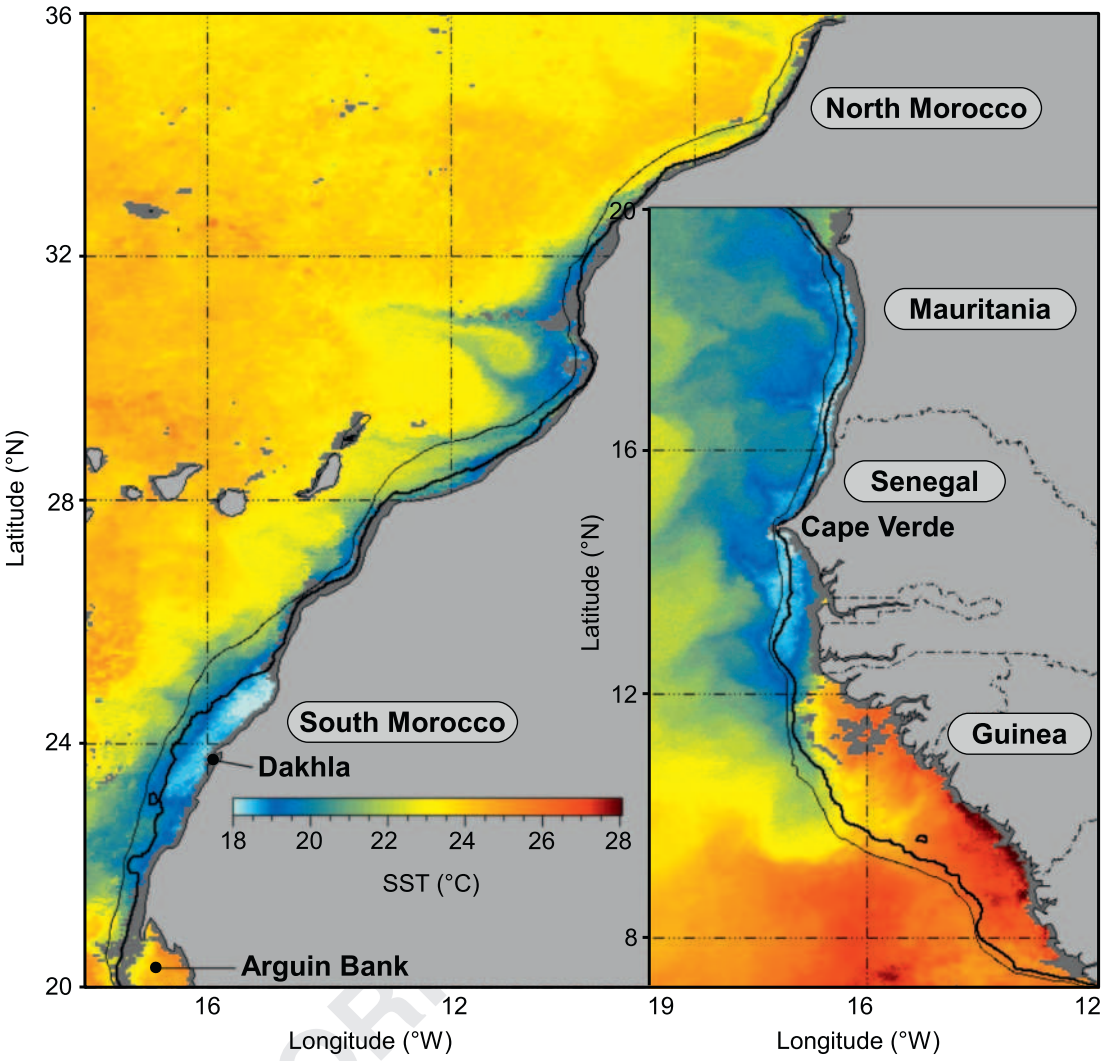

Fig. 3. 8-Day SST composites showing the spatial structure of the coastal upwelled waters in the Moroccan region (left panel) and in the southern part of the system, respectively in 01–08 August 2003 and 1–8 March 2006. The 50 m (thick line) and 200 m (thin line) isobaths are superimposed.

Waters. Without a very clear measure of SST_{up} (the original temperature of the upwelled water before it reaches the sea surface) this normalization was difficult to apply to the Moroccan region and introduced a seasonal bias.

Consequently, our contribution to the "classic" SST-based upwelling index is to improve the way the thermal difference is defined, taking into account the spatial structure of the upwelling and its link with the Ekman index.

The thermal difference between coastal and offshore SST is used to define the coastal upwelling index, thereafter noted CUI_{SST}, which is the simplest conceivable definition of an upwelling index exclusively based on SST. Practically, the CUI_{SST} has been defined as the thermal difference between the cold coastal water and the warmer offshore water at the same latitude. This thermal upwelling index was used by several authors, derived either from in-situ measurements (Wooster et al., 1976; Speth et al., 1978; Speth and Kohne, 1983; Mittelstaedt, 1983) or derived from satellite data (Mittelstaedt, 1991; Van Camp et al., 1991; Nykjaer and Van Camp, 1994; Santos et al., 2005; Lathurilère et al., 2008; Marcello et al., 2011; Santos et al., 2011) in order to estimate the latitudinal and temporal variability of the intensity of the upwelling. The general formulation is therefore very simple:

$$CUI_{SST\ (lat,\ time)} = SST_{offshore\ (lat,\ time)} - SST_{inshore\ (lat,\ time)}$$

At a given latitude and time, both SSTs respectively represent the offshore maximum and the inshore minimum SST that best define the cross-shore SST gradient. Nevertheless, the way both thermal references were chosen in the literature was always arbitrary. The consequence is double: first the resulting index was quantitatively questionable (i.e. for the same $SST_{inshore}$, a relatively short distance to select the $SST_{offshore}$ would generally decrease its value and consequently the index itself), second the latitudinal coherency of the index was affected by this choices. The challenge is therefore to study the best way to properly define and extract these two thermal references, (thereafter $SST_{inshore}$ noted as SST_{min} and $SST_{offshore}$ as SST_{max}) by using the remote sensing data in an adequate way.

3.2.1. *Reference for SST_{min}*

SST_{min}, the minimal local SST recorded in a cross-shore transect between the coast line and the continental slope, is the most obvious surface structure, easily identifiable from SST fields, either very close to the coastline (in case of narrow continental shelf) or more generally slightly separated from the coast. The accuracy in the estimation of the SST_{min} is closely dependent on the quality of the SST field and specially on its spatial resolution.

Consequently, at a given latitude, the SST_{min} is defined as the minimum SST recorded in the coastal band from the coast up to

Please cite this article as: Aïssa, B., et al., An improved coastal upwelling index from sea surface temperature using satellite-based approach –.... Continental Shelf Research (2014), http://dx.doi.org/10.1016/j.csr.2014.03.012

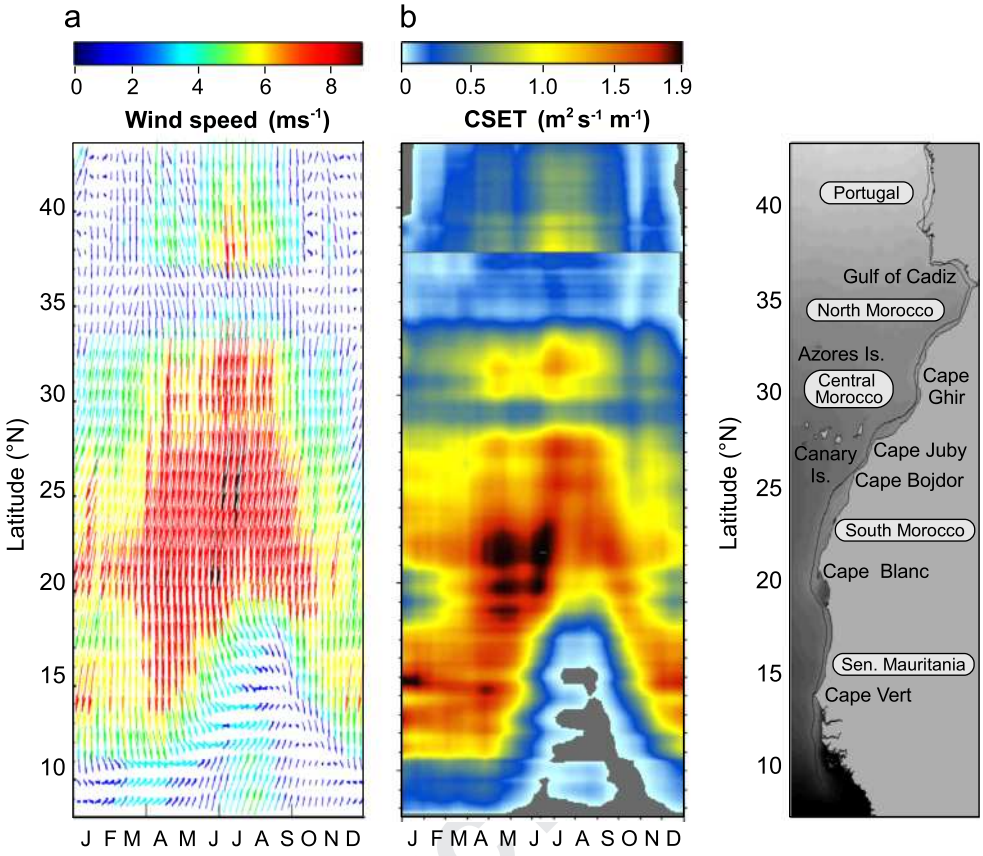

Fig. 4. (a) Climatological mean (8-day averages) of the CCMP satellite wind speed and direction, averaged from 50 to 150 km from the coast, for the period 1988–2010, (b) associated Cross-Shore Ekman Transport (CSET). The break at 37°N is due to the E–W coastline orientation of the northern part of the Gulf of Cadiz.

the distance of the continental slope. In order to minimize local noise in the data, SSTmin is averaged with the 8 pixels surrounding the exact location of the minimum.

In order to refine and secure the spatial determination of the SST_{min} – a value that could be highly impacted by the data quality – and to consider the invariant effects of the continental shelf geometry, all weekly situations are used to compute the spatial occurrence of the location of the upwelled waters, determined by the location of all SST_{min} for each coastal position and for each week of the year. The resulting positions are reported in term of probability of occurrence (Fig. 5a) as well as in monthly distance to the coast (Fig. 5c). In 25% of the cases, the SST_{min} cannot be identified in the 8-day averages because of clouds constraints.

In order to avoid possible spurious localisations of the SST_{min}, we only consider as realistic for further determinations of SST_{min} in individual weeks the area where 95% of the SST_{min} occurrence occur, explicitly considering both inshore and offshore limits of these positions.

3.2.2. *Definition of an optimal reference for SST_{max}*

SST_{max} is defined as the offshore temperature where the influence of the upwelling is supposed to be insignificant, in order to use it as a "thermal reference" of what would be the coastal SST without any upwelling. SST_{max} is processed from the current 8 day SST fields and not from the SST climatology. Two reasons explain this choice: firstly the 8-day compositing period of the SST fields is long enough to reduce the noise caused by the cloud coverage; Secondly, it integrates the influence of SST anomalies associated with large-scale climatic trends, independently of the upwelling process itself. Because it is defined to be independent of the upwelling itself, SST_{max} is latitudinally and seasonally dependent in a progressive way.

The offshore distance taken for SST_{max} is determined from the weekly climatology by maximizing the correlation between the climatological SST-based CUI_{SST} and the wind-based climatological CSET. In particular, a special attention is given to the maximization of the seasonal cycles by latitudinal areas, as detailed bellow.

All previous SST-based indices make use of various locations of SST_{max} at arbitrary distances from the coast, whereas the coastal reference itself is measured over various widths. Nykjaer and Van Camp (1994) choose the offshore position at 500 km from the coast, whereas the most coastal SST was systematically used as the SST_{min} reference. Carr and Kearns (2003) computed the SST difference at each 9 km pixel of their data set by subtracting the coastal SST, averaged over 1° of latitude and longitude, from the offshore SST at 5° further offshore at the same latitude. They consequently measured a continuous field of temperature differences when moving offshore. Santos et al. (2005) found that the general patterns of the spatio-temporal variability of their SST-based index were similar within the range 400–1000 km offshore. Lathurilère et al. (2008) chose the SST average in the band located within 500–700 km from the coast. For Marcello et al. (2011), the warm reference is also chosen at 500 km offshore, reproducing the same index as Nykjaer and Van Camp (1994). Zhaoyun et al. (2012) define their SST-based index for the Benguela upwelling ecosystem as $\Delta T \times A$, where A is an upwelling area defined as its coldest part (computed from a fuzzy C-mean clustering) and ΔT is the drop of temperature between this area and the ambient non-upwelling area, taken as the SST averaged from 9°E to the external coastal upwelling boundary at the same latitude.

In this work, we avoid the arbitrary choice of defining a fix position of the offshore SST reference (SST_{max}). At the contrary, we consider the seasonal dynamic of the upwelling as a suitable criteria to compare two upwelling indices, computed either from the Ekman theory or from SST, knowing that the thermal response

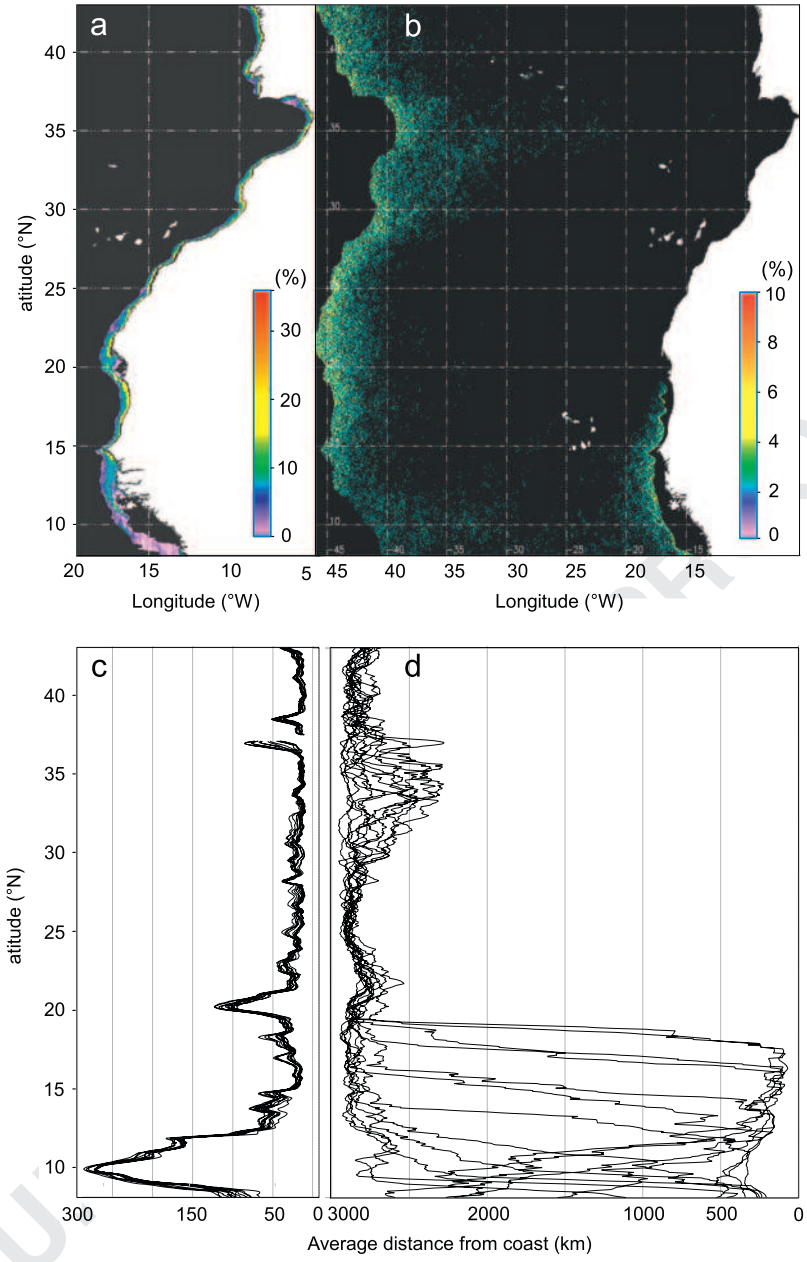

Fig. 5. (a) Spatial average probability of occurrence of the SST_{min}. The coastal band represents the area where 95% of the occurrences are observed (b) Probability of occurrence of the SST_{max} (c and d) Corresponding monthly distances, measured from the coast, highlighting their seasonal variability.

at the sea surface is only of a few days and in any case less than one week (Pelegrí et al., 2005).

So, despite their fundamentally different nature and irrespectively of their pro and cons, both indices are supposed to describe the same physical phenomenon and consequently to display similar seasonalities.

As a first attempt to set up an optimal distance for the SST_{max}, we use a fixed distance of 3000 km, that approximately corresponds to the center of the Atlantic Ocean.

The results (Fig. 5b and d) show that the resulting distances of the SST_{max} (here at a maximum distance of 3000 km) varies in latitude, mostly according the intensity of the upwelling. The distance tend to be naturally reduced between 30°N and 37°N, where the upwelling is less intense, and also south of 20°N where the upwelling is strongly seasonal. At the contrary, the distance tend to be closed to the maximum allowed limit when the upwelling is very intense, typically between 20 and 28°N.

This raises the question of the dynamic behind this observed variability, and the way a possible relationship with the upwelling intensity could be considered in the construction of the index itself. This step is detailed in the next paragraph.

3.2.3. *Relationship between the distance of SST_{max} and the upwelling index*

In order to simplify the following results, we use this first index to define distinct latitudinal regions by combining the characteristics of the CUI_{SST} and its seasonal amplitude, based on the previous 3000 km maximum distance. A split into five regions, from north to south is presented in Fig. 6: the Portuguese coast (43–37°N, excluding the northern part of the Cadiz area because of the East–West coastline orientation) characterized by a high and stable seasonality, the northern Morocco (33–36°N) characterized by a low seasonality and upwelling index, the central Morocco

Please cite this article as: Aïssa, B., et al., An improved coastal upwelling index from sea surface temperature using satellite-based approach –.... Continental Shelf Research (2014), http://dx.doi.org/10.1016/j.csr.2014.03.012

(26–33°N) with a progressively higher index and seasonality, the Southern Morocco region (21–26°N) with a high index and a very low seasonality, and the Senegal and Mauritania region, with a very high but decreasing seasonality associated to regularly decreasing upwelling indices. Very similar characteristics and limits between areas have been found using the CSET (for both wind data used), except for the 26°N limit that would have been shifted to 29°N, where a local minimum is noticed, as shown in Fig. 4b. This zonation is therefore more comprehensive and objective than those obtained by Nykjaer and Van Camp (1994), Makaoui et al. (2005) and Santos et al. (2005).

Based on this zonation, we optimized the search of the best maximum range for SST_{max}, by exploring the seasonal correlations between both indices, the CUI_{SST} and the CSET (derived from both QuikSCAT and CCMP). SST_{max} is successively chosen as the warmest SST found between a short distance from the coast (250 km) up to a maximum distance of 3000 km, by step of 250 km.

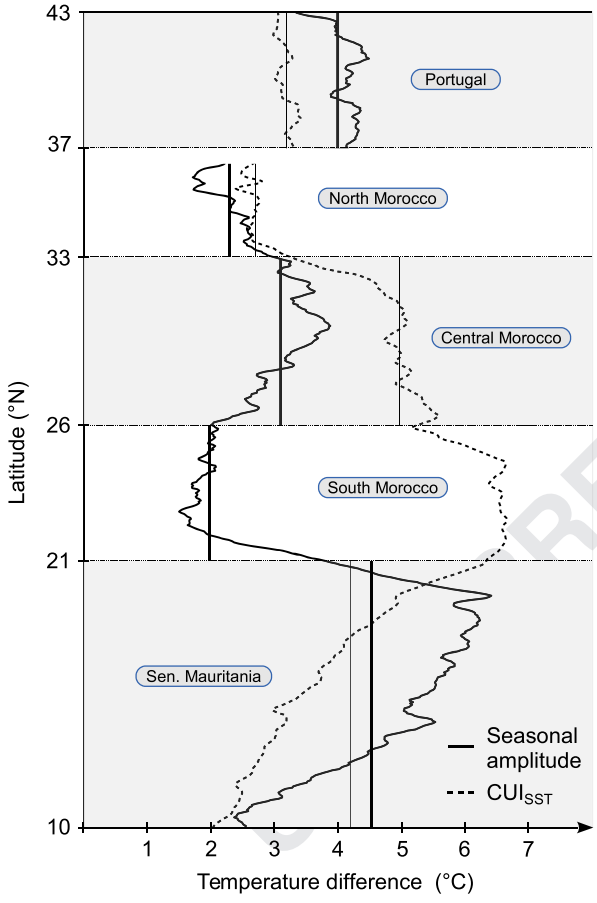

Fig. 6. Latitudinal classification of the upwelling activity into five areas, based on the average value of their thermal zonal difference (CUI_{SST}) and its seasonal amplitude, both expressed in °C. The vertical bars help to visualize the average values of the parameters.

The results are computed for four of the previous latitudinal regions (Table 1), each maximum distance corresponding to a different measurement of CUI_{SST}. Except for the northern Morocco region that do not show interpretable results because of its low seasonality, each area shows an increasing correlation with the distance to the coast, with systematically better correlations with CCMP than QuikSCAT wind. For Portugal, the correlation regularly increases up to a distance of 1750 km in northern Morocco and 3000 km in the central and southern Morocco. For the last region (9–21°N), where the SST seasonality is very pronounced, a high and flat correlation is found (between 0.86 and 0.92), closer to the coast, between 1000 and 3000 km.

As previously thought, the increasing correlations up to a maximum that occurs at various distances, clearly suggest a deterministic link between the upwelling intensity and the distance where the SST is supposed to be independent of the upwelling activity. This link is represented by the statistical relationship between the distance found for the SST_{max} and the upwelling index (Fig. 7a). All individual observations ($n=1365$, gray cloud) as well as their deciles ($n=136$, black points) show a fairly stable relationship, across seasons and latitude, adjusted by a fourth-degree polynom.

In a second step, the whole time series has been reprocessed, in order to force the maximum location of the SST_{max} according to the intensity of the upwelling given by this average relationship. The result (Fig. 7c) shows a more robust result, with a clearer latitudinal and seasonal evolution of the position of the SST_{max}.

The rapid change observed when we move from tropical to subtropical waters (Fig. 6d) is induced by the universal mechanism of the upwelling process. When the upwelling is permanent and very intense, the dilution of the coastal upwelled waters progressively affects a larger marine area (as seen in Fig. 2b), pushing further offshore our SST_{max} reference. The width of this area also depends on the cumulative effect of the upwelling intensity, nevertheless the average intensity of the coastal upwelling gives a good approximation of this maximum distance, as confirmed by the relationship obtained.

The distance of the SST_{max} reference is very moderate (less than 500 km) for upwelling index <1.5 °C and then rapidly increases to values over 2000 km for CUI_{SST}.of 3 °C (vertical line on Fig. 7a) to progressively reach a plateau up to maximum values close to 2750 km.

At lower latitudes (11–21°N), the CUI_{SST} index varies from very low to very high values and this variability is well reflected through the corresponding SST_{max} distances (Fig. 7b and c) that seasonally varies from 300 to 2800 km. In the southern part of this region, the summer intrusion of the Guinean warm water force the SST_{max} to be even closer from the coast, reinforcing even more the previous effect. Q5

Table 1
Correlation between the seasonal cycle of the CUI_{SST} and the CSET derived from QuikScat and CCMP wind for four different regions, computed for variable distances of SST_{max}, from 250 to 3000 km to the coast. The highest coefficients (± 0.01) are highlighted in bold.

Offshore distance (km)		250	500	750	1000	1250	1500	1750	2000	2250	2500	2750	3000
Area	**Wind**												
37.5–43°N	**QSC**	0.16	0.21	0.30	0.32	0.35	**0.36**	**0.37**	**0.38**	**0.37**	0.35	0.31	0.30
	CCMP	0.21	0.28	0.37	0.39	0.44	**0.46**	**0.47**	**0.48**	**0.48**	0.45	0.39	0.34
26–33°N	**QSC**	−0.07	−0.01	0.07	0.09	0.18	0.27	0.31	0.34	0.39	0.46	**0.48**	**0.49**
	CCMP	−0.04	0.03	0.10	0.11	0.21	0.31	0.36	0.40	0.46	0.53	**0.55**	**0.55**
21–26°N	**QSC**	0.01	0.03	−0.08	−0.11	−0.15	−0.07	−0.02	0.11	0.22	0.33	0.41	**0.47**
	CCMP	−0.06	−0.04	−0.12	−0.16	−0.19	−0.11	−0.04	0.08	0.19	0.29	0.38	**0.45**
9–21°N	**QSC**	0.75	0.80	0.83	**0.86**	**0.87**	**0.86**	**0.86**	**0.86**	**0.85**	**0.85**	**0.85**	**0.86**
	CCMP	0.80	0.86	0.90	**0.92**	**0.93**	**0.93**	**0.92**	**0.92**	**0.92**	**0.92**	**0.92**	**0.92**

Please cite this article as: Aïssa, B., et al., An improved coastal upwelling index from sea surface temperature using satellite-based approach –.... Continental Shelf Research (2014), http://dx.doi.org/10.1016/j.csr.2014.03.012

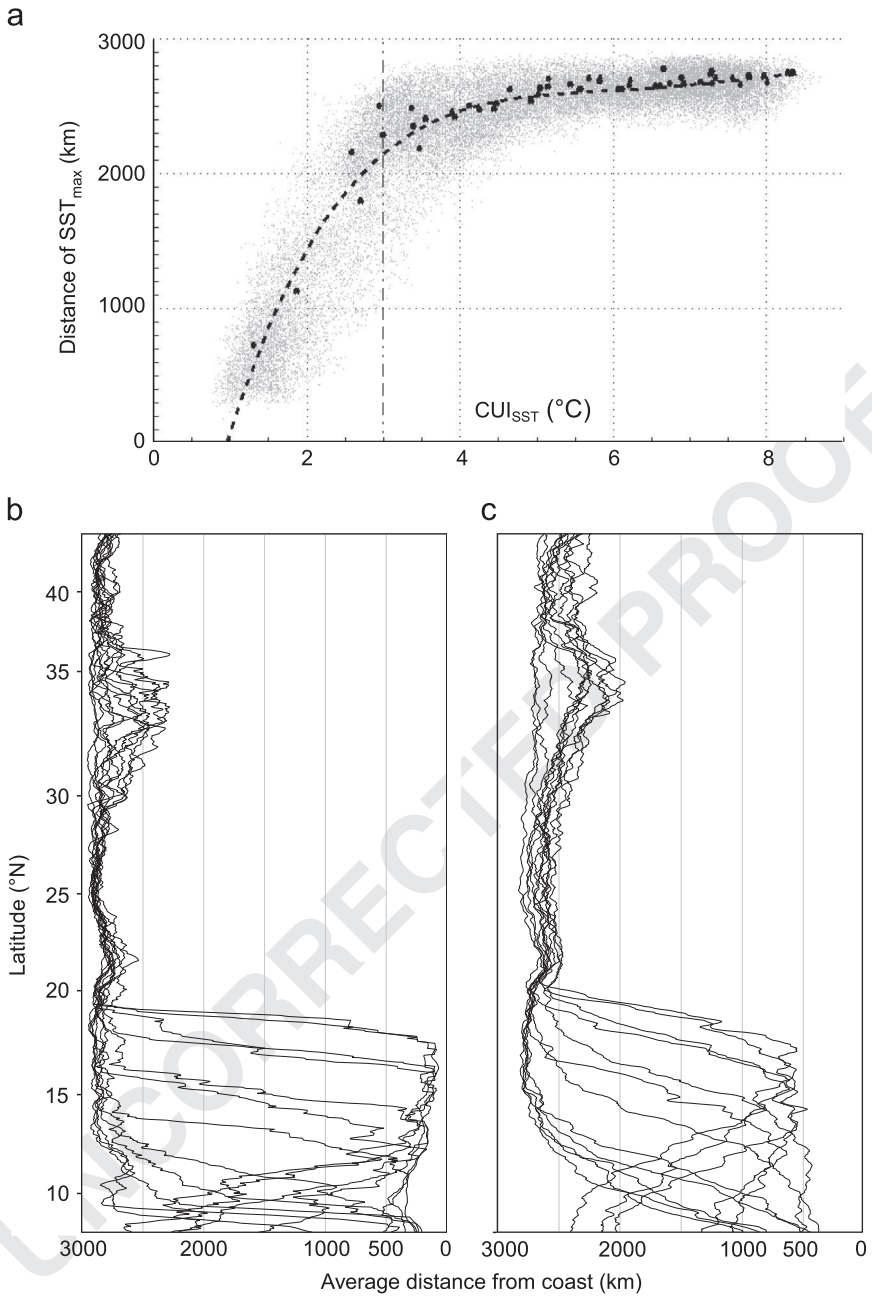

Fig. 7. (a) Statistical relationship between the distance of the SST_{max} (found at a maximum distance of 3000 km) and the corresponding SST-based upwelling index. Raw values are in gray and the black dots represents the deciles for each of the five areas previously defined. The adjustment (dashed line) is computed by a fourth-degree polynom. (b and c) Climatological distances of SSTmax respectively before and after the application of the relationship obtained in (a).

At mid-latitude (21–33°N), isotherms are vertically structured by the wide Canary Current flow (Fig. 2b) that moves parallel to the coastline (Wooster et al., 1976).

4. Results

4.1. Seasonal pattern of SST_{min} and SST_{max}

The seasonal variability of the observed SST_{min} (Fig. 8a) strongly varies latitudinally because it depends first on the seasonality of the heat exchanges with the atmosphere, and second on the intensity of the upwelling itself, that also varies seasonally.

Because they result from the interplay between these two parallel processes, the absolute values of SST_{min} have little signification by themselves and only their seasonality is described here.

In the same line, it has been noted that the surface temperature of the upwelled water, as measured from numerous cruises in the Moroccan coastal waters (Makaoui et al., 2005), is effectively seasonally varying, even for the same upwelling intensity, as computed from the local wind.

As shown from the average value of these minimal temperatures in space and time (Fig. 8a), a band of relatively low seasonality is depicted in the northern part of the system (21°N–43°N), because the summer upwelling strongly reduces the normal seasonal amplitude of the SST at these latitudes, as observed further offshore from the SST_{max} (Fig. 8b). This effect is maximal when the upwelling is very strong in summer (21–25°N) with the weakest seasonal amplitude of the whole system, 2.5 °C, observed at 21.5°N.

Between 33°N and 37°N, the weaker summer upwelling (because of weaker winds and unfavorable coast line orientation) results in a

Please cite this article as: Aïssa, B., et al., An improved coastal upwelling index from sea surface temperature using satellite-based approach –.... Continental Shelf Research (2014), http://dx.doi.org/10.1016/j.csr.2014.03.012

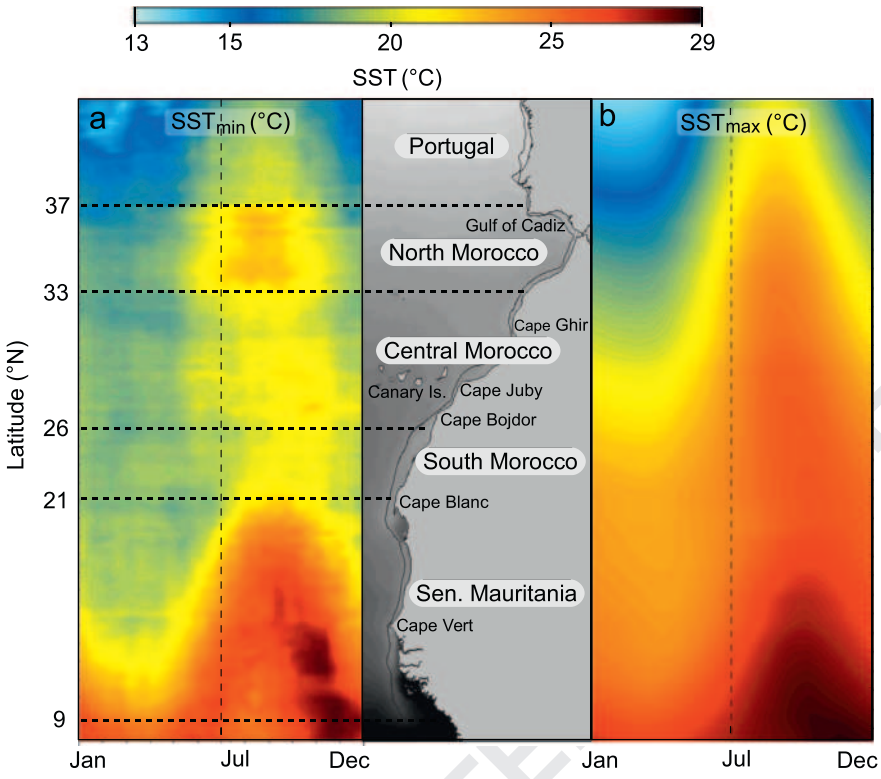

Fig. 8. (a) Space-time Hovmoller plot of the average values of the SST_{min} and (b) the SST_{max} recorded from 1981 to 2011and used for the CUI_{SST} index.

relatively higher SST_{min} seasonality, that converges again towards the SST_{max}.

At the contrary, in the southern part of the system (8–21°N), the winter upwelling strongly enhances the seasonal thermal contrast, with amplitudes higher than 7 °C between 13°N and 17°N.

The climatological SST_{max} reference (Fig. 8b) displays a seasonality that varies in a regular sinusoidal way for all latitudes according the air–sea heat fluxes, confirming that this reference is quasi independent of the upwelling influence.

4.2. *Seasonal spatio-temporal variability of the CUI_{SST} index*

The seasonal variability of the upwelling intensity is described by the CUI_{SST} index for the Canarian upwelling system via the same space-time diagram, at a 4-km/8-day spatio-temporal resolution, from 8°N to 43°N (Fig. 9a). The original data is smoothed with a 3-term moving average in time (24 days), and a 5-term moving average in space (22 km). The result shows a high spatio-temporal definition of the patterns of upwelling intensity, with well defined seasonal transitions, generally associated to Capes (Cape Ghir, Cape Juby, Cape Bojdor), sometimes permanently (Cape Blanc).

The seasonal variability is tightly associated with the meridional position of the trade winds, which affects the northern part of the region in summer and its southern part in winter, following the seasonal movement of the ITCZ (Wooster et al., 1976; Speth et al. 1978; Speth and Kohne, 1983).

In the southern part of the system (Senegal, Mauritania and Guinea) the seasonality is enhanced by the rapid replacement of the trade winds by monsoon winds in June, which advected the warm Guinean water northward in the coastal region. During winter and spring (December to May), this region and the southern Moroccan region (21°N–26°N) tend to merge to form a spatially continuous upwelling region, characterized by the strongest intensity of the whole Canary system (upwelling index >7 °C).

Q6 Contrary to previous observations (i.e. Marcello et al., 2011), the whole area (9–43°N) appears to be permanently or seasonally submitted to the upwelling activity; i.e., the upwelling index is positive everywhere (except for an interruption at the Strait of Gibraltar).

The main patterns of variability are synthesized into the five characteristic regions previously defined (Fig. 9b). These areas can be easily grouped into three regions of variability as previously described by Santos et al. (2005): northern summer upwelling, permanent central upwelling and southern winter upwelling.

In the first group, from north to south, the northern Portuguese region (37.5–43°N), the Northern (33–36°N) and Central (26–33°N) Moroccan regions show similar seasonal patterns (dashed lines in Fig. 9(b)) characterized by a pronounced summer maxima between August and early September, and from north to south to an increasing upwelling intensity associated to a decreasing seasonal amplitude. The Portuguese area displays high summer average intensity (6.7 °C) and the highest average seasonality (4.5 °C) of this part of the system. The Northern Morocco shows the weakest upwelling (intensity between 2 °C and 4.5°), mainly because of weaker winds (see Fig. 4a) and an unfavorable orientation of the coast line. In the Central Morocco region, the upwelling is much stronger (summer maximum of 7.4 °C near Cape Ghir) with a moderate seasonal amplitude of 3.2 °C.

The Southern Moroccan region (21–26°N) is characterized by a strong and quasi-permanent upwelling and trade winds (Fig. 4a), with only two relative minimum in March and August, due to residual influence of the seasonal minimum of the trade winds in winter in the northern part of the system and in summer in its southern part.

Last but not least, the Senegalese–Mauritanian region (9–21°N) shows a wide and pronounced winter maximum (5.8 °C) and a seasonal amplitude of 3.9 °C. These average climatic values are close to their northern equivalent, (Portugal), except that the seasonal amplitude can reach locally 6 °C on average.

Outside the Canary upwelling system, the summer coastal cooling of Guinea–Liberia is visible. This feature has been considered as the northernmost extension of the southern coastal upwelling system of Ivory Coast and Ghana, whose influence is known to reach the

Please cite this article as: Aïssa, B., et al., An improved coastal upwelling index from sea surface temperature using satellite-based approach –.... Continental Shelf Research (2014), http://dx.doi.org/10.1016/j.csr.2014.03.012

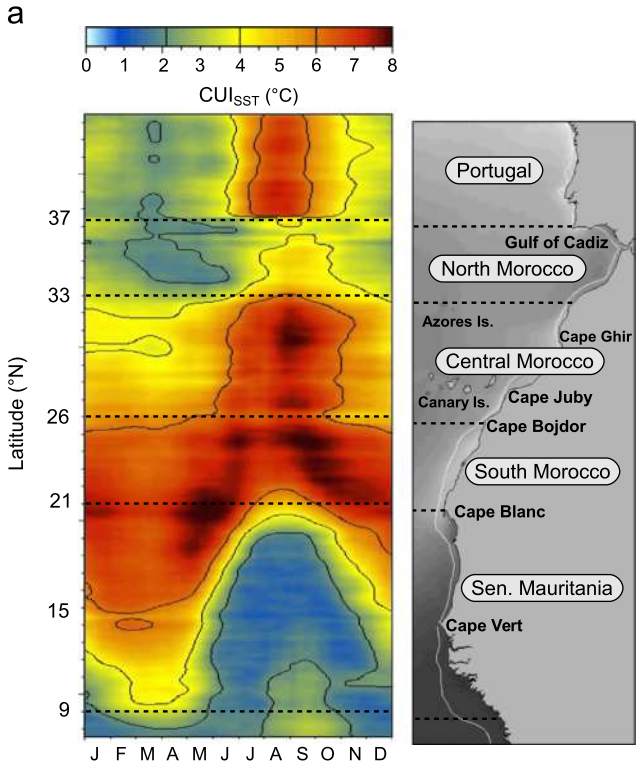

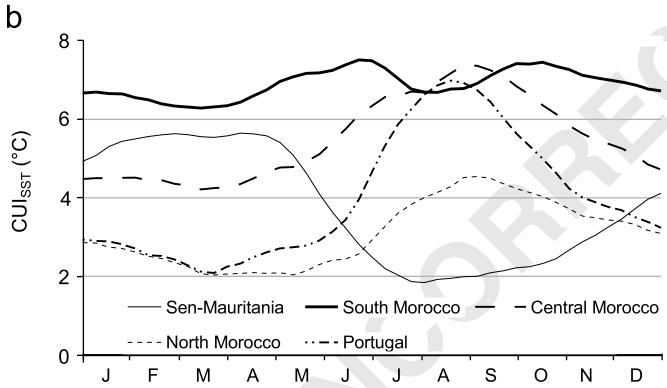

Fig. 9. (a) Space-time Hovmoller plot of the CUI$_{SST}$ index computed from the 1981–2011 time series. Values 2, 4 and 6 °C are contoured. (b) Seasonal variability (three weeks moving average) of the CUI$_{SST}$ index for the five characteristic areas (Portugal: 37.5–43°N, North Morocco: 33–36°N, Central Morocco:26–33°N, South Morocco: 21–26°N and Senegal–Mauritania: 9–21°N) of different intensity and seasonality of the index.

northern Guinean coast and to create a measurable negative SST anomaly (Berrit, 1962).

4.3. Comparison of the upwelling index with previous SST-based indices

We compared our upwelling index (Fig. 10c) with the result obtained using the method described in Marcello et al. (2011), first with similar colors as originally published (Fig. 10a), then with same colors and scale than our index (Fig. 10b), in order to facilitate the comparison. The SST-based index computed by Nykjaer and Van Camp (1994) is not presented because of its extreme similarity to Marcello's index.

The comparison reveals very large differences in term of upwelling intensity, between 1 and 4 °C according areas. Our index (CUI$_{SST}$) pics at 8 °C between 21°N and 25°N while the Marcello's index do not exceed 4 °C in the same region which lead to an underestimation of the upwelling intensity of 50%. Another consequence of the Marcello index is the negative average values found north of 33°N. This is due to the constant and arbitrary distance of 750 km taken as the oceanic SST reference. This distance is undoubtedly too short, specially in the central part of the system where the oceanic influence of the upwelled waters reaches at least 2000 km. At the opposite, this distance is too large between 9 and 21°N where the summer coastal intrusion of the warm Guinean water off the continental shelf generates negative upwelling indices (in white on Fig. 10b), during summer, where the upwelling is very weak but not negative. A similar anomaly is observed in spring and summer for the Northern Moroccan region, where observed wind patterns (Fig. 4a) are consistent with a weak coastal upwelling. The highest differences are observed at 20°N from March to July, where the warm inshore waters of the Arguin bank lead to a severe bias in the determination of the coastal SST minimum.

It is therefore evident that a careful spatial determination of both thermal terms is a central point in computing an accurate SST-based upwelling index. As a consequence, the use of the same satellite data set (in this case the AVHRR pathfinder series) can lead to very different results according the methodology used, and also that the very first definitions of SST-based upwelling index by Wooster et al. (1976) and Speth et al. (1978), established before the era of satellite observation by subtracting measured coastal SST values to mid ocean or zonal averaged SST at the same latitude, was already a very significant step in that direction.

4.4. Comparison with cross-shore Ekman transport

The intensity and seasonal dynamic of our SST-based upwelling index, CUI$_{SST}$, (Fig. 11a) is compared with its Ekman equivalent (CSET) computed using two different wind sources: SeaWinds/QuikSCAT (Fig. 11b) and the CCMP product (Fig. 11c). The spatio-temporal map of the differences between CUI$_{SST}$ and CSET$_{CCMP}$, is also produced (Fig. 11d). At large scale, the seasonal patterns are very similar. The differences are mostly about the duration of the upwelling season, specially regarding its decreasing phase. Both indices have nearly coincident maxima and minima, leading to a global positive correlation, as previously quantified. A time lag is observed between both variables (Table 2), probably due either to different inertia between the atmosphere forcing and the ocean response, or to advective processes. The lag is maximum in the central sub-area (26–33°N) where it can reach 7 weeks, and minimum in the southern-most region (9–21°N) with a value between 3 and 4 weeks.

The differences between both normalized indices (Fig. 11d) show that the CUI$_{SST}$ is generally higher, in the sense that the thermal upwelling period appears to be longer. The fact that the SST-based index is fundamentally a measure of a coastal cooling makes that other processes than Ekman upwelling, like horizontal advection are automatically "added" as a contribution to the observed cooling. In the other hand, the CSET index is based on the Ekman theory (Ekman, 1905) which assumes an infinite and homogeneous ocean and a constant wind. Therefore, the intensification of the coastal upwelling in the vicinity of capes and the influence of submarine canyons or ridges is not reflected in the Ekman index (Nykjaer and Van Camp, 1994).

5. Discussion

5.1. Spatial considerations

The spatial variability of the coastal upwelling structure is explored, with a special focus on the effects of the bathymetry. The Fig. 3 shows typical spatial patterns of the upwelled waters, for the Moroccan region (left panel) and the Senegalese–Mauritanian region (right panel), respectively during summer (August) and late winter

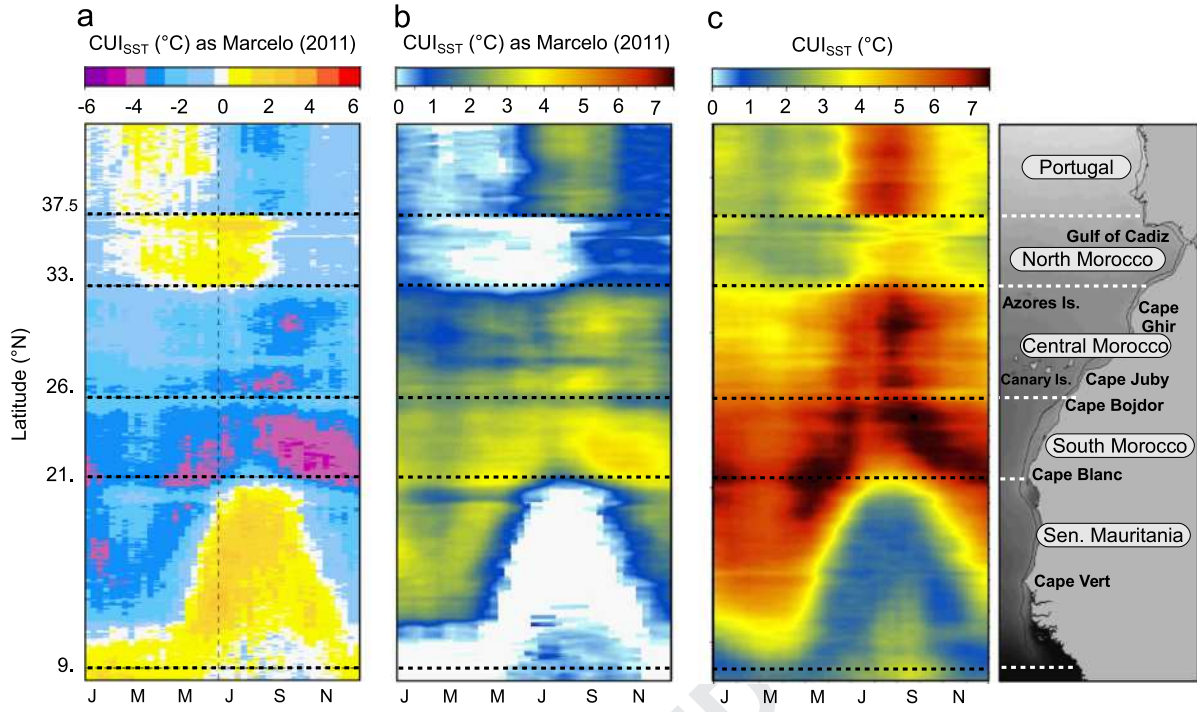

Fig. 10. Climatological Coastal Upwelling Index based on coastal and offshore SST difference for the period (1987–2006) as produced by Marcello (2011) with (a) their original colors (b) enhanced colors with negative values in white and (c) computed with our own methodology, with the same scale and colors.

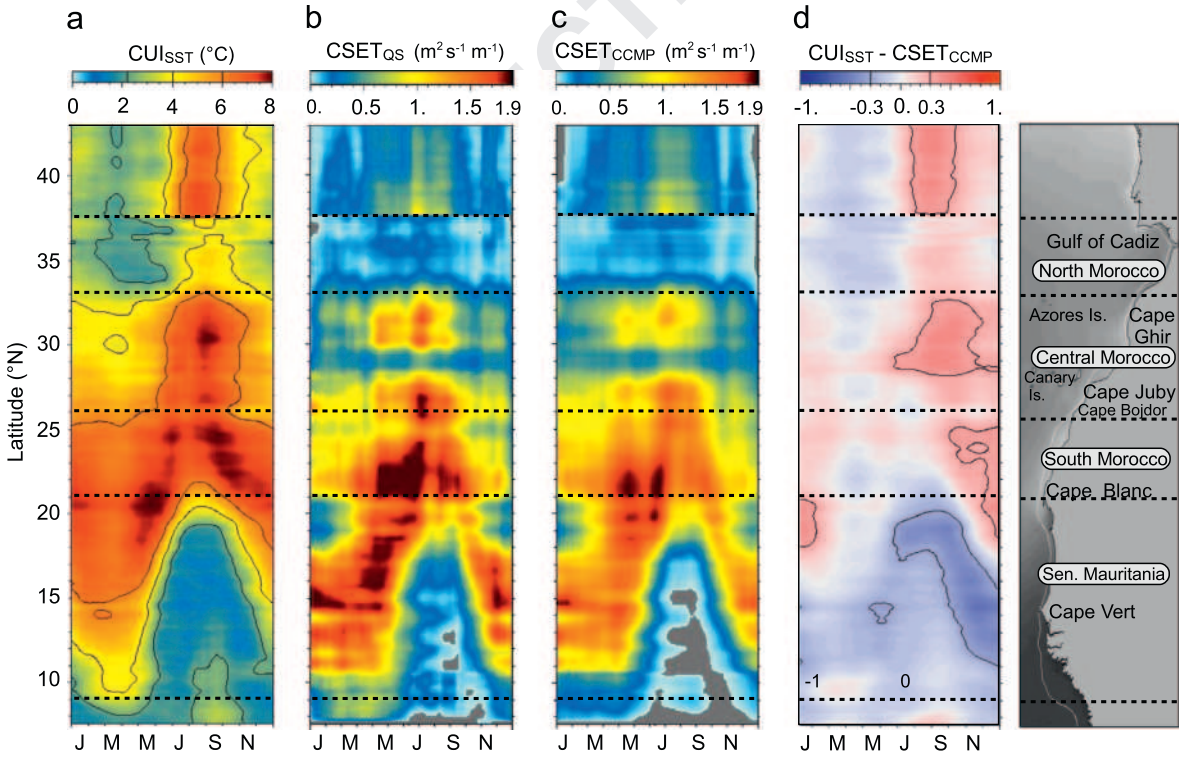

Fig. 11. Seasonal variability of (a) CUI$_{SST}$, (b) and (c) CrossShore Ekman Transport (CSET) computed respectively from QuikSCAT and CCMP winds, (d) normalized differences between CUI$_{SST}$ and CUIC$_{CMP}$.

(March) when the upwelling reach its respective maximum latitudinal extensions.

It has been shown (Fig. 5a) that there is little variability in the spatial location of the upwelled waters, and a very strong relationship with the bathymetry.

From north to south, the North and Central Morocco regions (Fig. 3 left panel) show that the thermal minimum is almost as close to the coast than physically detectable – and always in the 0–50 m bathymetry range – even in regions (32°N and 28°N) where the continental shelf is slightly wider. In the Southern Morocco region, this is confirmed by the statistical occurrences (Fig. 5a) where it is shown that most of the detections are close to the coast, even if some are also found more offshore. This behavior has been previously observed from in-situ data (Barton et al., 1977;

Please cite this article as: Aïssa, B., et al., An improved coastal upwelling index from sea surface temperature using satellite-based approach –.... Continental Shelf Research (2014), http://dx.doi.org/10.1016/j.csr.2014.03.012

Walsh et al., 1977) with the observation of a secondary surface cooling, sometimes observed at the vicinity of the continental slope. This is also in accordance with previous observations of Jacques and Tréguer (1986) that noted for wide continental shelf regions of West Africa a double upwelling cell circulation, one close to the coast, that usually dominates and a secondary one at the vicinity of the continental slope and whose relative importance increases with the upwelling intensity.

In Senegal and Mauritania (Fig. 5c) the patterns are different, still in accordance with the bathymetry. The Arguin bank show more variable positions of the SST_{min} in its northern part, probably due to the change in the orientation of the continental slope, whereas in its southern part, the steepest slope is acting as a guide, with the coldest water always found very close to the 50 m isobath. This behavior is confirmed by the statistical occurrences of SST_{min} (Fig. 5a) always found between the 50 m and 200 m isobaths. Further south, the SST_{min} is regularly closer to the coast (confirmed in Fig. 5a), in close accordance with the progressively narrower shelf, up to the latitude of Cape Verde. Then the width of the shelf increases to reach a maximum between 10 and 11°N in the Guinean region. The width of the continental shelf itself has no direct influence on the location of the thermal minimum, but it is clear that the steepness of the continental slope, well defined by the proximity of both 50 m and 200 m isobath, acts as a guide for the emergence of the upwelled waters at the sea surface. Active upwellings winds are observed in March as south as 8°N (and probably more, see Fig. 2a), and a significant surface cooling is effectively observed in late winter (February–March) in this region (Fig. 2b), up to 7°N.

This coastal cooling can not be attributed to the Ekman pumping, since none of the satellite wind data show upwelling favorable winds at this period of the year. At the contrary, slightly negative values of Ekman transport would indicate a slight downwelling. This coastal cooling was already noted by Berrit (1962) who observed from in-situ measurements a seasonal amplitude of SST of 5 °C at the latitude of Cape Vergas, in Guinea at 10.5°N. This latitude was considered as the northernmost location of the southern coastal upwelling system of the Guinea Gulf, that occurs between July and September (Berrit, 1962), when the ITCZ reaches its northernmost position. This feature is enhanced by the Guinea Dome, formed by the combined action of the superficial North equatorial counter Current (NECC, see Fig. 1) and the northern deviation of the North Equatorial Under Current (NEUC), that supply the southern part of the Canarian system (up to the latitude of Cape Blanc) with the rich South Atlantic Central Water (SACW), as described in Voituriez (1981).

A careful search of this summer surface cooling on the AVHRR 8-day averages shows that a cold surface signature is effectively visible, mostly in September and October (Fig. 12) between 10 and 12°N, the latitude of the Guinea dome in this season (Voituriez and Dandonneau, 1974), whose eastern part probably enhance the coastal branch of the NECC, creating a local divergence and a significant surface cooling of several degrees Celcius (between 1 and 2 °C in the monthly averages).

If it is clear that the use of higher spatial resolution data set (nominally 1.1 km) would improve the precision of the determination of the local SST minimum, both in space and intensity. It is however evident that, independently of the spatial limitation, the quality of the cloud mask is of primary importance for an optimal determination of this minimum. The standard masking procedures are effectively very far for perfect in highly dynamic areas and specially in the Canary upwelling system. A specific constraint is the application of a "reference test", consisting in the flagging of cold water that is 2 °C colder that the climatology (See Kilpatrick et al., 2001 for details). This effect, well visible in the SST fields of Fig. 3 (and even more on average in all 8-day composited), is detrimental to a precise determination of the thermal coastal minimum. It is therefore evident than the reference to a climatology should be reconsidered.

Nevertheless, the previous spatial considerations have greatly improved the way the minimum coastal SST values have been determined, improving the computation of the SST-based upwelling index.

Table 2
Correlations between CUI_{SST} and two different CSET derived from QuikScat and CCMP wind data, for different time lags (in weeks) for four regions.

Area\time-lag		0	1	2	3	4	5	6	7	8
37.5–43°N	**QSC**	0.35	0.47	0.51	0.52	**0.56**	**0.57**	0.55	0.57	0.57
	CCMP	0.45	0.56	0.64	0.68	**0.71**	**0.70**	0.67	0.67	0.63
26–33°N	**QSC**	0.46	0.52	0.55	0.61	0.68	0.71	**0.76**	0.73	0.68
	CCMP	0.53	0.59	0.62	0.66	0.66	**0.69**	**0.70**	0.68	0.63
21–26°N	**QSC**	0.33	0.37	0.34	0.37	0.39	0.37	**0.41**	0.37	0.35
	CCMP	0.29	0.32	0.31	0.37	0.36	0.37	**0.40**	0.37	0.34
9-21°N	**QSC**	**0.85**	0.84	0.82	0.77	0.70	0.61	0.53	0.43	0.32
	CCMP	**0.92**	0.90	0.87	0.82	0.75	0.66	0.57	0.47	0.37

5.2. Comparison between CCMP and QuikSCAT wind

CCMP wind analyses from composite products where used in this study, because they cover the longest part of the study period. When compared to high quality single sensor products, as the SeaWinds on board QuikSCAT, some important discrepancies were observed in space and time between both products, specially prior to 2001, when the QuikSCAT winds where not integrated into the CCMP product. This is explained by the starting estimate used in the variational

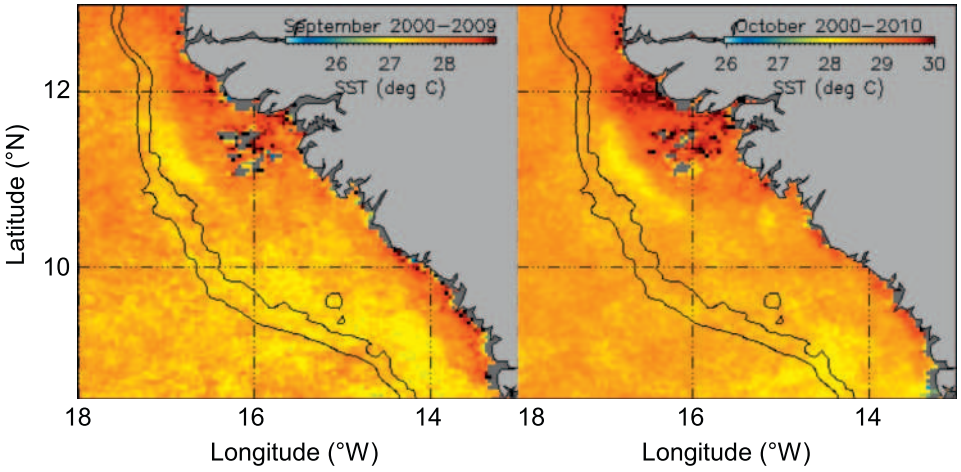

Fig. 12. SST averages in September and October in the Guinean region (2000–2010 period) showing the presence of an upwelling structure between 10 and 12°N.

analysis method of the CCMP product, changing from the ECMWF Reanalysis for July 1987 until December 1998 to the ECMWF Operational Analysis used from January 1999 onward, with an increase spatial resolution (Atlas et al., 2009). Until today, only one recent study (Carvalho et al., 2013) has compared CCMP, QuikSCAT and buoy winds recorded during one full year, in 2008. The results do not show major differences between CCMP and QuikSCAT, except a tendency of QuikSCAT to overestimate the wind speed. This result is in agreement with our comparison of the seasonal cycle of the CSET derived both from CCMP and QuikSCAT (Fig. 11b and c), this later showing a systematic positive bias for the highest wind speeds.

The interannual comparison of the SST-based and the Ekman CSET indices computed from both winds data sets during the 2000–2008 period (Fig. 13) shows contrasted results. In central Morocco (Fig. 13a), differences between both CSET indices are weak, except in summer during the upwelling season, where the indices derived from QuikSCAT are significantly higher than those from CCMP wind but also closer to our thermal index. In the Mauritania–Senegalese area (Fig. 13b) the CCMP wind is close to our index, specially in 2000 and 2001, a period during which QuikSCAT gives much higher indices than CCMP, with a progressive attenuation from 2000 to 2006.

It is interesting to note that there is no unique relationship between SST-based and wind-based indices, and this relationship slightly changes according regions.

All together, noticeable differences appear between products according regions and time periods and precise conclusions would require quality meteorological measurements. Nevertheless, It is therefore important to compare several data sets on the longest possible period in order to evaluate possible uncertainties between wind products as well as between indices that aim to describe the same phenomenon.

The CCMP wind, presently the longest high quality data set available for our study period, is on average closer to our index, specially in term of seasonal amplitude.

5.3. Interannual variability of CUI_{SST}

The space-time diagram of the SST based coastal upwelling index (CUI_{SST}) computed from the weekly 8-day SST (Fig. 14) shows the seasonal and interannual variation of the west African upwellings for the 30 years from July 1981 to December 2011. It highlights the latitudinal variations in upwelling intensity and seasonality, as well as in terms of spatio-temporal extent.

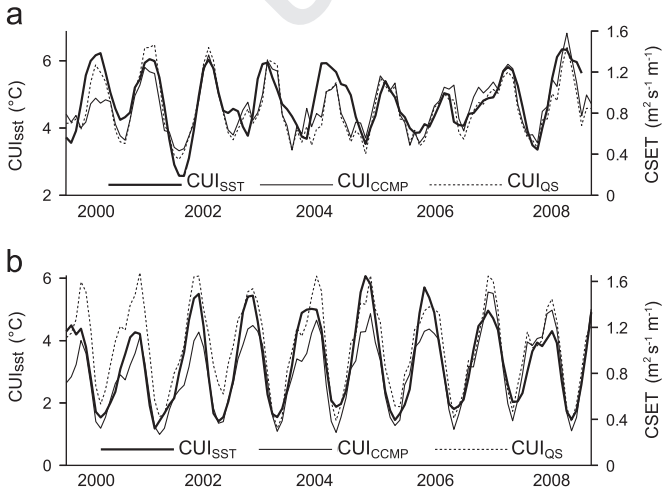

Fig. 13. Comparison of the variability of the CUI_{SST} (plain lines) and the CSET computed respectively from the CCMP wind (thin lines) and the QuikSCAT wind (dotted lines) from 2000 to 2008 for (a) the Central Morocco and (b) the Senegal–Mauritania region. Both CSET series are 3-term averaged.

The five regions previously defined are still very distinct, with the greatest intensity occurring in southern Morocco (21°–26°N) where the upwelling is quasi permanent, followed by the central Morocco (26–33°N) in summer and the Mauritanian–Senegal area in winter.

The interannual variability is more pronounced in the central and northern part of the system with well defined continuous latitudinal anomalies. Between 9 and 21°N (Mauritania–Senegal), the anomalies are sometimes in phase with the northern part of the system (i.e. in 1999) but sometimes completely out of phase, as in 1996.

The whole time period was characterized by a considerable year to year variability and oscillations between periods of strong (1982, 1984, 1991, 1993, 1996, 1998, 1999, 2002, and 2005) and weaker upwelling (1983, 1987, 1989, 1990, 1994, 1995, 1997, 1998, 2001, 2005, 2006 and 2009). Nevertheless, such separation is very area depending and only few years present clear anomalies for the whole system, as 1998–99 or 2008–2009, where a North to South propagation of the high upwelling intensity is visible. Alternatively, several exceptional upwelling seasons were found for only part of the system, for example very weak intensities were observed from end the end of 1995 to 1997 in the Moroccan part of the region (Figs. 14, 15a–b), related to exceptional relaxations of the trade winds. This strong anomalies have been associated to a quasi absence of juveniles in 1996 and 1998 and the collapse of the regional sardine stock between 1996 and 1997 (Machu et al., 2009). At the contrary, some years are associated to strong upwelling seasons only in the southern part of the system as in 1986, 1996, 1999, 2005, 2009 and 2011.

The Southern Morocco region (Fig. 15b) is characterized by a constantly high upwelling activity, with a wind maximum in summer and a thermal minimum associated to a time lag of 5–6 weeks (not shown) for an average correlation of 0.31. Such a correlation is very depending of the length of the time series and this numbers should be considered with extreme care. The important fact is that some periods shows similar temporal patterns between indices, as in 1991, between 1998 to 2003 and in 2010. Important differences also occur for years where the thermal index is comparatively much lower, as for the 1994–1996 and 2006–2009 periods. Such discrepancies can be due either to horizontal advective processes or to an inadequate cloud masking (that prevent a valid minimum SST to be detected), both effects occurring in this region.

In the Mauritania–Senegal area, (Fig. 15c) both indices are fully in phase which means that the upwelling is tightly linked to the seasonality of the trades winds, without time lag (Table 2).

The influence of the variability of the NAO index is also explored for two Moroccan regions and Portugal from 1982 to 2011 (Fig. 16). During this period, large variations of the NAO index are observed, with a general decrease of its average intensity after 1995 followed by values close to zero in 1996–97 and extreme negative values in 2010–11. The high index observed in 1994 was also reported by Hurrell (1995) and Santos et al. (2005).

This decreasing trend of the NAO is not reflected in the upwelling indices, but all extreme events of 1983, 1994, 1996–97, 1999 and 2010–11 are well visible in the CUI_{SST} series (gray bars on Fig. 16) for the three areas.

This result show that the NAO definitively plays an important role in the extreme upwelling events observed, but not on the long term variability of winds Nevertheless, a similar number of NAO events are negatively reflected by our index (hatched bars), as in 1984–85, 1988-89, 1992, 2001–02, 2004 and 2007.

This complex behavior is well reflected by the low and poorly significant seasonal correlations between NAO and our index for the Center and Southern Morocco (Table 3, last line), as well as between NAO and meridional wind component (Table 3, first line).

Please cite this article as: Aïssa, B., et al., An improved coastal upwelling index from sea surface temperature using satellite-based approach –.... Continental Shelf Research (2014), http://dx.doi.org/10.1016/j.csr.2014.03.012

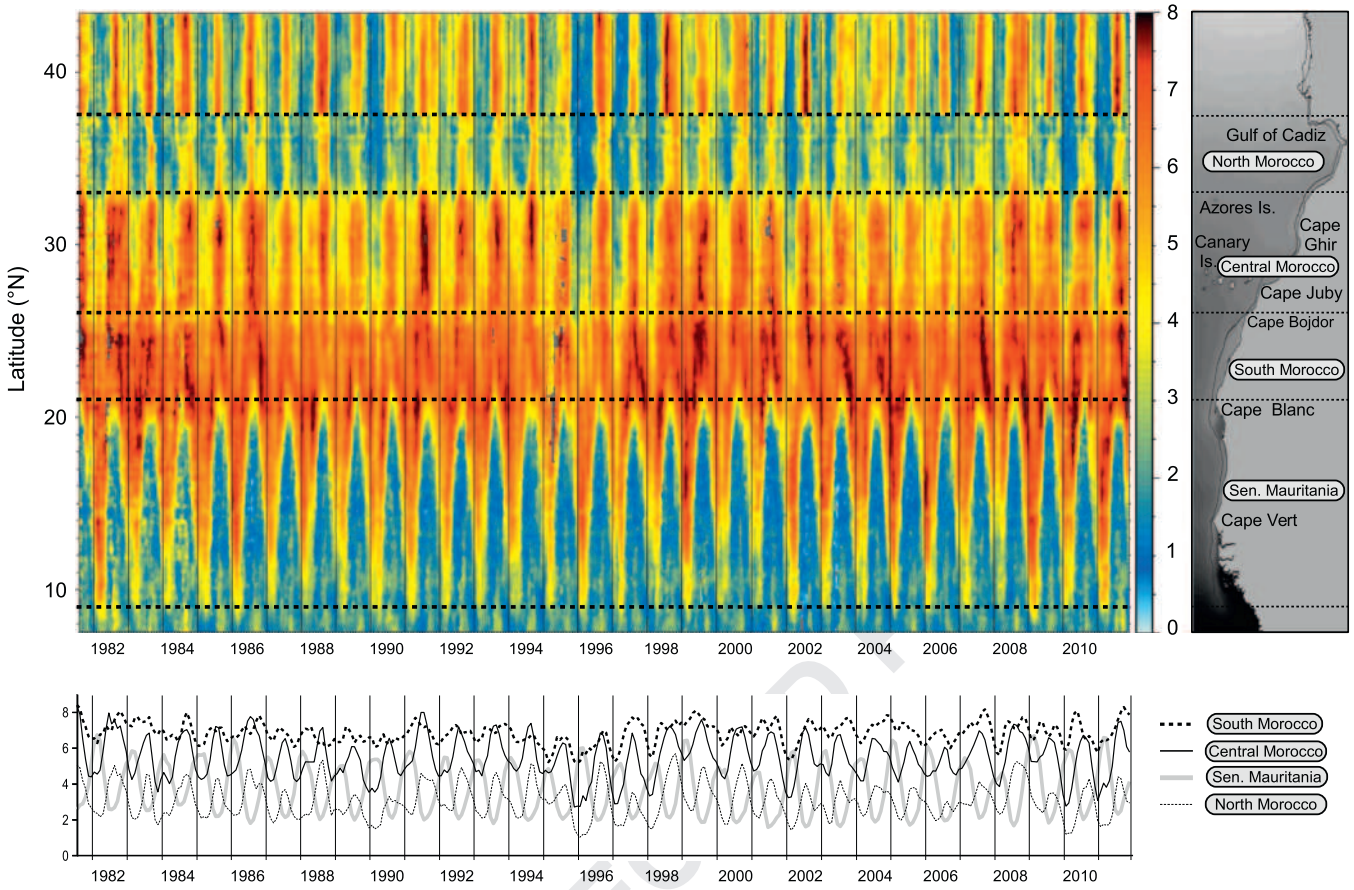

Fig. 14. Space-time Hovmoller plot of the seasonal and interannual variability of the CUI_{SST} (upper panel) from 1982 to 2011 and monthly time series of the four characteristic areas previously identified, (lower panel).

Not surprisingly, we also note the seasonal correlations between meridional Wind and CUI_{SST} are much higher and always significant (Table 3, line 2) for all seasons and both areas, with the highest value ($r=0.53$) observed in autumn for the central Morocco. This shows that a systematic link between atmospheric pressure differences and upwelling-favorable wind is far to be established, whatever the type of upwelling index used.

5.4. Considerations about a thermal upwelling index

An SST-based upwelling index should not be reduced to an alternative to a wind-based index but rather as a complementary assessment of the local resulting impact of the coastal upwelling process. Because there is several ways to compute and SST-based index and because a thermal superficial effect is the result of several processes, including currents and topographical constraints, it is shown here that there is no universal relationship between both indices. At the contrary, they strongly varies between the five regions of the Canary upwelling system (as shown by Fig. 15), and in particular, the thermal inertial effect of the upwelled waters through the year is clearly visible when the upwelling is strong and its seasonal duration important. This is the case in the Central Morocco in 1996 (Fig. 15a), at the end of the upwelling season (i.e. from 1990 to 1994), because of the inertia of the water masses. At the contrary, inverse time lags also exist (i.e. for years 2005 to 2009) when the wind precedes the surface cooling. This effect is negligible in Senegal and Mauritania, because of the shorter upwelling season (less thermal inertia) and the rapid arrival of the Guinean water after the upwelling season.

Another crucial point about upwelling indices, whatever the spatio-temporal scale and methodology used, is the type and quality of the input data, either SST or wind. The accuracy of cloud masking procedures of satellite infrared data can strongly impacts the final SST product quality, and consequently the accuracy of coastal SSTs. This issue, discussed earlier, is crucial for our purpose. Another constraint for assessing the quality of SST-based upwelling indices and consequently to promote their use in environmental studies is their comparison with well established indices, i.e. Ekman upwelling indices, specially for long time series, for which homogeneous data sets often do not exist. For the 30 last years, this is a serious problem, even regarding the use of meteorological wind data, whose homogeneity is not guaranteed, due to changes in measure instrument or local constraints. Contrarily to SST, this is the case for satellite wind data for which most missions do not exceed 10 years (the longest ones are from the SSM/I microwave sensor on board the DSMP satellites). For this reason, important differences are sometimes found between both types of indices. This is the case in central Morocco before 2000 (Fig. 15a), where the CSET computed with CCMP wind was surprisingly low compared to the CUI_{SST}, with a difference of almost 2 °C reported in the CUI_{SST} scale. This is not the case afterwards, where both indices were comparatively very close. This raises the question of the use of composite winds for indices comparisons, when their quality changes with the integration of different quality data, as the QuikSCAT winds from 2000. This also gives us a relatively higher confidence in our SST-based index computed from the same original data set, as a consistent thermal response of the local wind forcing computed.

Because of its very different nature, the thermal-based upwelling index must not be assimilated to a classic upwelling index (in term of water flow) but as one of its superficial effect. In counterpart, its biological meaning is important for numerous marine species, whose physiology and habitat is closely depending

Please cite this article as: Aïssa, B., et al., An improved coastal upwelling index from sea surface temperature using satellite-based approach –.... Continental Shelf Research (2014), http://dx.doi.org/10.1016/j.csr.2014.03.012

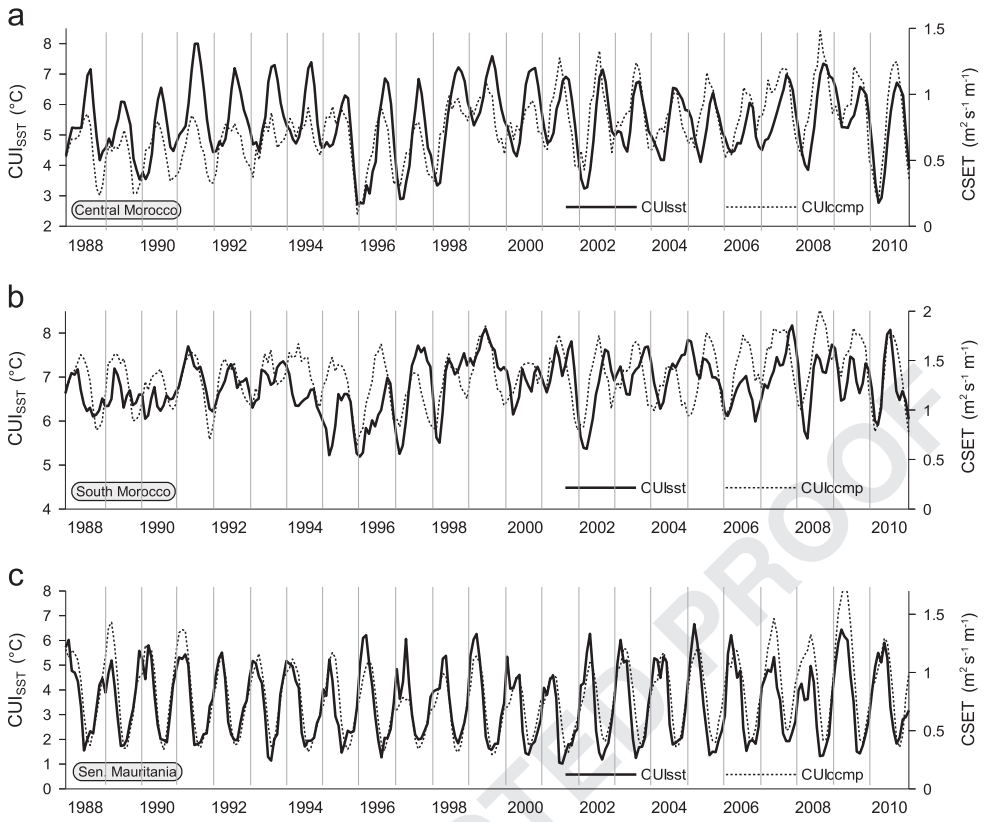

Fig. 15. Comparative seasonal and interannual variability of the CUI_{SST} (plain lines) and the CSET from the CCMP wind (doted lines) from 1988 to 2010 for three contrasted areas: (a) Central Morocco, (b) South Morocco and (c) Senegal–Mauritania. The time step is monthly and the CSET is 3-term averaged.

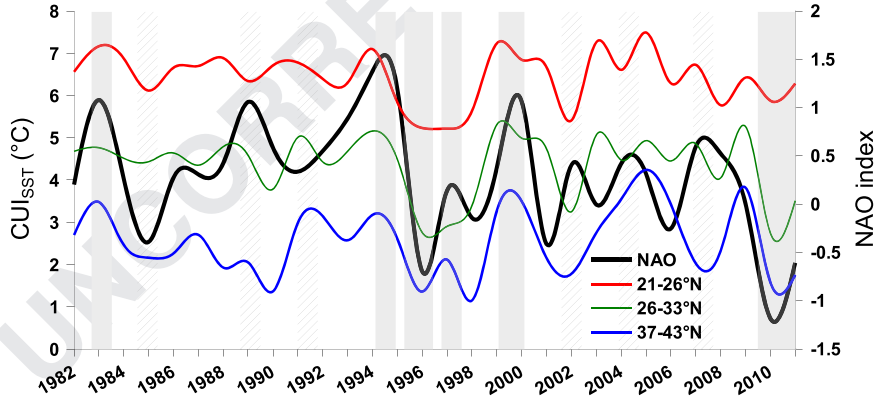

Fig. 16. Comparison of the variability of the CUI_{SST} in southern and central Morocco and Portugal (colored lines) with the North Atlantic Oscillation index (black line) from 1982 to 2011.

Table 3
Correlations by seasons between the North Atlantic Oscillation index (NAO) and the meridional wind component (V_{wind}) and SST-based upwelling index (CUI_{SST}) for two different areas characterized by a seasonal upwelling (Central Morocco, 26–33°N) and a permanent upwelling (Southern Morocco, 21–26°N).

	Winter	Spring	Summer	Autumn
NAO/V_{wind}	Center: **−0.13***	Center: **0.19***	Center: *0.04*	Center: *−0.05*
	South: **−0.11***	South: *−0.02*	South: *−0.04*	South: *−0.06*
V_{wind}/CUI_{sst}	Center: **−0.45*****	Center: **−0.25***	Center: **−0.43****	Center: **−0.53*****
	South: **−0.49*****	South: **−0.31***	South: **−0.13***	South: **−0.41****
NAO/CUI_{sst}	Center: **−0.26***	Center: *0.06*	Center: **−0.16***	Center: *0.07*
	South: *0.02*	South: **−0.17***	South: **−0.22***	South: *−0.05*

* Significant levels at 5%.
** Significant levels at 1%.
*** Significant levels at 0.1%.

on the resulting cooling (among other properties) of the coastal upwelling. Another property of this index is its ability to describe in great detail (depending of the intrinsic quality of the SST product used) some observed spatial characteristics of the coastal upwelling, as its origin and spatial extent, both very dependant on local bathymetric constraints.

Please cite this article as: Aïssa, B., et al., An improved coastal upwelling index from sea surface temperature using satellite-based approach –.... Continental Shelf Research (2014), http://dx.doi.org/10.1016/j.csr.2014.03.012

6. Conclusion

The proposed SST-based upwelling index is not only a satisfying alternative to the Cross-shore Ekman transport, it supplies a complementary description of the upwelling physical properties, in particular independent measurements of its intensity and thermal inertia, that varies in space and time with intensity and duration. Detailed patterns of the variability of the Canary upwelling are reproduced, that integrates useful informations on the complexity of the effects of both bathymetry and advective processes.

Extensive comparisons with along-shore wind stress computed from QuikSCAT and CCMP data, and with previous SST-based indices allow us to evaluate these differences in term of seasonal and interannual variability in the Canary system.

The improvement over simplest SST-based indices was first to improve the extraction procedure of the minimal SST reference and, more importantly, to determine an optimal offshore thermal reference, both by considering the relationships between its intensity and spatial components.

Further improvements are now very dependant of the quality of the cloud discrimination, far from perfect for pathfinder data in the Canary upwelling system because of the overestimation of the cloud cover over upwelling cells, limiting the quality of the coastal SST retrieval and therefore the precision of SST-based upwelling indices. The use of higher spatial resolution data (nominally 1.1 km) is a way to partly overcome these limitations.

An important point when computing upwelling indices is the consistency of the data quality over time. This is not the case for AVHRR pathfinder data but this question remains open for composite products such as the CCMP wind data, at least at some locations and periods.

By providing a generic way to compute coastal upwelling indices, our revised methodology helps to monitor coastal upwelling ecosystems, where satellite data is generally abundant. As demonstrated in recent years, early warning signal of the upwelling intensity will help resource managers to determine the probability of abrupt changes that impact fish catches. In Morocco, fisheries are managed by quarterly quotas based on acoustic surveys of INRH (Institut National de Recherche Halieutique), with an additional support in the form of a monthly bulletin (INRH, 2013) that describes the main oceanic and atmospheric variables, including the present SST-based upwelling index.

Q2 Uncited references

Hagen et al. (1996).

Acknowledgments

Q7 We applied the FLAE approach for the sequence of authors. We thank the 50th Anniversary Young African fellowship programme of IOC (Intergovernmental Oceanographic Commission) as well as the French Institute of Research for Development (IRD) for partially supporting this work. The SST data were provided by GHRSST and the US National Oceanographic Data Center, in a project partly Q8 supported by a grant from the NOAA Climate Data Record (CDR). QuikSCAT and CCMP global wind were obtained from the NASA Physical Oceanography Distributed Active Archive Center at the Jet Propulsion Laboratory.

We are grateful to collegues Larissi Jamila and Makaoui Ahmed for their helpful discussions about the comparison of our results with the in-situ data, as well as to Naoki Tojo comments that substantially improved the manuscript.

Last but not least, we are very grateful to two anonymous reviewers whose comments greatly improves the manuscript.

References

Arístegui, J., Barton, E.D., Álvarez-Salgado, X., Santos, M., Figueiras, F., Kifani, S., Hernández-León, S., Mason, E., Machu, E., Demarcq, H., 2009. Sub-regional ecosystem variability in the Canary Current upwelling. Prog. Oceanogr. 83, 33–48.

Atlas R., Hoffman R.N., Ardizzone J., Leidner S.M., Jusem J.C., 2009, Development of a new cross-calibrated, multi-platform (CCMP) ocean surface wind product. In: Proceedings of AMS 13th Conference on Integrated Observing and Assimilation Systems for Atmosphere, Oceans, and Land Surface (IOAS-AOLS).

Bakun, A., Nelson, C.S., 1991. The seasonal cycle of wind stress curl in subtropical eastern boundary current regions. J. Phys. Oceanogr. 21, 1815–1834.

Bakun, A., 1973. Coastal upwelling indices, west coast of North America, 1946–71. U. S. Dep. Commer. 103 (NOAA Technical Report, NMFS SSRF-671).

Barton, E., Hayer, D., A., Smith, R.L., 1977. Temporal variability observed in the hydrographic regime near Cabo coreiro in the nortwest Africa upwelling region Februry to April 1974. Deep Sea Res. 24, 7–23.

Barton, E., 1998. Eastern boundary of the North Atlantic: Northwest Africa and Iberia. Coastal Segment (18, E).. In: Robinson, A.R. (Ed.), The Sea, vol. 11. John Wiley and Sons, New York, pp. 633–657.

Benazzouz A., 2014. Upwelling Côtier et Effet de la Dynamique Océanique à Méso-Échelle Sur la Variabilité Planctonique Dans le Système du Courant des Canaries (Ph.D. thesis). Hassan II Mohammedia-Casablanca University.

Berrit, G.R., 1962. Contribution à la Connaissance des Variations Saisonnières dans le Golfe de Guinée: Observations de Surface le Long des Lignes de Navigation. ORSTOM Ed, Pointe-Noire (33 pp.).

Campbell, J.W., Blaisdell, J.M., Darzi, M., 1995. Level-3 SeaWiFS Data Products: Spatial and Temporal Binning Algorithms, vol. 32; (73 pp.).

Carr, M.E., Kearns, E., 2003. Production regimes in four Eastern Boundary Current systems. Deep-Sea Res. II 50, 3199–3221.

Carvalho, D., Rocha, A., Gómez-Gesteira, M., Alvarez, I., Silva Santos, C., 2013. Comparison between CCMP, QuikSCAT and buoy winds along the Iberian Peninsula coast. Remote Sens. Environ. 137, 173–183.

Cushing, D.H., 1971. Upwelling and the production of fish. Adv. Mar. Biol. 9, 255–334.

Demarcq, H., Faure, V., 2000. Coastal upwelling and associated retention indices derived from satellite SST. Apllication to *Octopus vulgaris* recruitement. Oceanol. Acta 4, 11231–11246.

Ekman, V., 1905. On the influence of the earth's rotation on ocean-currents. Ark. Mat., Astron. Fys. 2, 1–53.

Freilich, D.G., Long, Spencer, M.W., 1994. SeaWinds. A scanning scatterometer for ADEOS II science overview. In: Proceedings of the International Geoscience and Remote Sensing Symposium, Pasadena, CA, IEEE, pp. 960–963.

Fiuza, A., de Macedo, M.E., Guerreiro, M.R., 1982. Climatological space and time variation off the Portuguese coastal upwelling. Oceanol. Acta 5, 31–40.

Fréon, P., Barange, M., Aristegui, J., 2009a. Eastern boundary upwelling ecosystems: integrative and comparative approaches. Prog. Oceanogr. 83, 1–14.

Hagen, E., Zülicke, C., Feistel, R., 1996. Near-surface structures in the Cape Ghir filament off Morocco. Oceanol. Acta 12 (6), 577–598.

Hagen, E., 1981. Mesoscale upwelling variations off the West African coast. In: Richards, F.A. (Ed.), Coast. Upwelling. American Geophysical Union, Washington, pp. 72–78.

Herbland, A., Voituriez, B., 1974. La production primaire dans l'upwelling mauritanien en mars 1973. Cah. O.R.ST.OM., Sér. Océanogr. 12 (3), 187–201.

Hurrell, J.W., 1995. Decadal trends in the North Atlantic Oscillation: regional temperatures and precipation. Science 269, 676–679.

Hurrell, J.W., 1996. Influence of variations in extratropical wintertime teleconnections on Northern Hemisphere temperature. Geophys. Res. Lett. 23 (6), 665–668.

INRH, 2013. Bull. Natl. d'upwelling 6(10 pp.).

Jacques, G., Tréguer, P., 1986. Ecosystèmes Pélagiques Marins. Masson(243 pp.). Q9

Kilpatrick, K.A., Podesta, G.P., Evans, R., 2001. Overview of the NOAA/NASA advanced very high resolution radiometer pathfinder algorithm for sea surface temperature and associated matchup database. J. Geophys. Res. 5, 9179–9197.

Kostianoy, A.G., Zatsepin, A.G., 1996. The West African coastal upwelling filaments and cross-frontal water exchange conditioned by them. J. Mar. Syst. 7 (2–4), 349–359.

Lathurilère, C., Echevin, V., Lévy, M., 2008. Seasonal and intraseasonal surface chlorophyll-a variability along the northwest African coast. J. Geophys. Res. 113, C05007, http://dx.doi.org/10.1029/2007JC004433.

Machu, E., Ettahiri, O., Kifani, S., Benazzouz, A., Makaoui, A., Demarcq, H., 2009. Environmental control of the recruitment of sardines (*Sardina pilchardus*) over the western Saharan shelf between 1995 and 2002: a coupled physical–biogeochemical modelling experiment. Fish. Oceanogr. 18 (5), 287–300.

Makaoui, A., Orbi, A., Hilmi, K., Zizah, S., Larissi, J., Talbi, M., 2005. L'upwelling de la côte atlantique du Maroc entre 1994 et 1998. Comptes Rendus Geosci. 337 (16), 1518–1524.

Marcello, J., Hernandez-Guerra, A., Eugenio, F., Fonte, A., 2011. Seasonal and temporal study of the northwest African upwelling system. Int. J. Remote Sens. 32, 1843–1859.

Q10
McClain, C.R., Yeh, E., Fu, G., 1992. An analysis of GAC sampling algorithms: a case study. In: Hooker, S.B., Firestone, E.R. (Eds.), NASA Goddard Space Flight Center, Greenbelt, Maryland, p. pp. 22.
Minas, H.J., Codispoti, L.A., Dugdale, R.C., 1982. Nutrients and primary production in the upwelling region off Northwest Africa. Rapp. P.-V. Reun., Cons. Int. Explor. Mer 180, 148–183.
Mittelstaedt, E., 1983. The upwelling area off Africa – a description of phenomena related to coastal upwelling. Prog. Oceanogr. 12, 307–331.
Mittelstaedt, E., 1991. The ocean boundary along the northwest African coast: circulation and oceanographic properties at the sea surface. Prog. Oceanogr. 26, 307–355.
Naderi, F.M., Freilich, M.H., Long, D.G., 1991. Spaceborne radar measurement of wind velocity over the ocean—an overview the NSCAT scatterometer system. Proc. IEEE 79, 850–866.
Nieto, K., Demarcq, H., McClatchie, S., 2012. Mesoscale frontal structures in the Canary upwelling system: new front and filament detection algorithms applied to spatial and temporal patterns. Remote Sens. Environ. 123, 339–346.
Nykjær, L., Van Camp, L., 1994. Seasonal and interannual variability of coastal upwelling along northwest Africa and Portugal from 1981 to 1991. J. Geophys. Res. 99 (C7), 14197–14207.
Pelegrí, J.L., Arístegui, J., Cana, L., González, M., Hernández-Guerra, A., Hernández-León, S., Marrero-Díaz, A., Montero, M.F., Sangrá, P., Santana-Casiano, M., 2005. Coupling between the open ocean and the coastal upwelling region off Northwest Africa: Water recirculation and offshore pumping of organic matter. J. Mar. Syst. 54, 3–37.
Peters, H., 1976. The spreading of the water masses of the Banc d'Arguin in the upwelling area off Northern Mauritanian Coast. "Meteor" Forschungsergeb. (A) 18, 78–100.
Reynolds, R.W., Smith, T.M., Liu, C., Chelton, D.B., Casey, K.S., Schlax, M.G., 2007. Daily high-resolution blended analyses for sea surface temperature. J. Clim. 20, 5473–5496.
Ryther, J.H., 1969. Photosynthesis and fish production in the sea. Science 166, 72–80.
Santos, M.P., Kazmin, A.S., Peliz, A., 2005. Decadal changes in the canary upwelling system as revealed by satellite observations: their impact on productivity. J. Mar. Res. 63, 359–379.
Santos, F., Gomez Gesteira, M., deCastro, M., Alvarez, I., 2011. Differences in coastal and oceanic SST trends due to the strengthening of coastal upwelling along the Benguela Current system. Cont. Shelf Res., 79–86, http://dx.doi.org/10.1016/j.csr.
Speth, P., Detlefsen, H., Sierts, H.W., 1978. Meteorological influence on upwelling off Northwest Africa. Dtsch. Hydrogr. Z. 31, 95–104.
Speth, P., Kohne, A., 1983. The relationship between sea surface temperatures and wind off Northwest Africa and Portugal. Oceanogr, Tropical 18, 69–80.
Trenberth, K.E., Large, W.G., Olson, J.G., 1990. The mean annual cycle in global ocean wind stress. J. Phys. Oceanogr. 20, 1742–1760.
Van Camp, L., Nykjaer, L., Mittelstaedt, E., Schlittenhardt, P., 1991. Upwelling and boundary circulation off northwest Africa as depicted by infrared and visible satellite observations. Prog. Oceanogr. 26, 357–402.
Voituriez, B., 1981. Les sous-courants équatoriaux nord et sud et la formation des dômes thermiques tropicaux. Oceanol. Acta 4 (4), 497–506.
Voituriez, B., Dandonneau, Y., 1974. Relations entre la structure thermique la production primaire et la regeneration des sels nutritifs dans le Dôme de Guinee. Cahiers O.R.S.T.O.M. Série Oceanogr. 13, 241–255.
Walsh, J.J., Whitledge, T.E., Kelle, J.C., Huntsman, S.A., Pillsbury, R.D., 1977. Further transition states of the Baja California upwelling ecosystem. Limnol. Oceanogr. 22, 264–280.
Wooster, W.S., Bakun, A., McLain, D., 1976. The seasonal upwelling cycle along the eastern boundary of the North Atlantic. J. Mar. Res. 34 (2), 131–141.
Zhaoyun, C., Xiao-hai, Y., Young-heon, J., Lide, J., Yuwu, J., 2012. A study of Benguela upwelling system using different upwelling indices derived from remotely sensed data. Cont. Shelf Res. , http://dx.doi.org/10.1016/j.csr.2012.05.013.

Please cite this article as: Aïssa, B., et al., An improved coastal upwelling index from sea surface temperature using satellite-based approach –.... Continental Shelf Research (2014), http://dx.doi.org/10.1016/j.csr.2014.03.012